Mean field and full field modeling of dynamic and post-dynamic recrystallization: application to 304L steel

PhD defense of Ludovic Maire

November 23rd, 2018

Supervised by:
Marc Bernacki, Nathalie Bozzolo, Charbel Moussa

Table of contents

Context of the study

Hot forming → **microstructure** → **final properties**

(www.sassda.co.za)

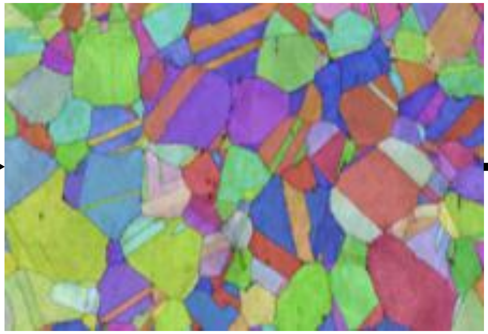

(Bobin et al., 2015)

- During hot deformation :
  - ➢ dynamic recrystallization (DRX) occurs
- After hot deformation :
  - ➢ post-dynamic recrystallization (PDRX) occurs

Dynamic Recrystallization (DRX)

Initial microstructure

STRAIN HARDENING

DYNAMIC RECOVERY + NUCLEATION

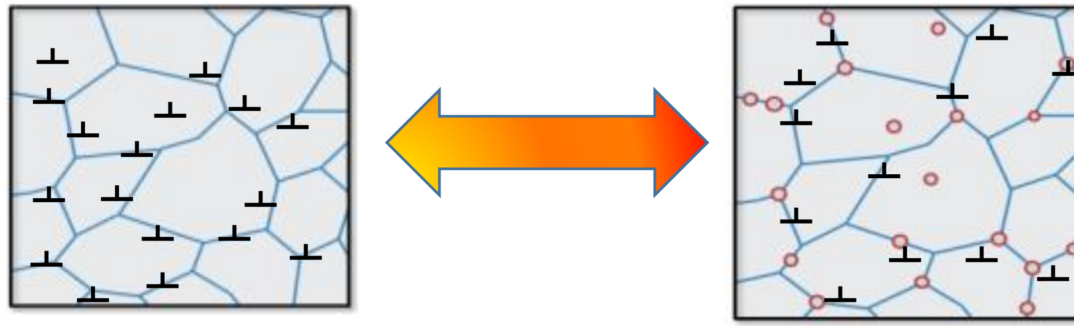

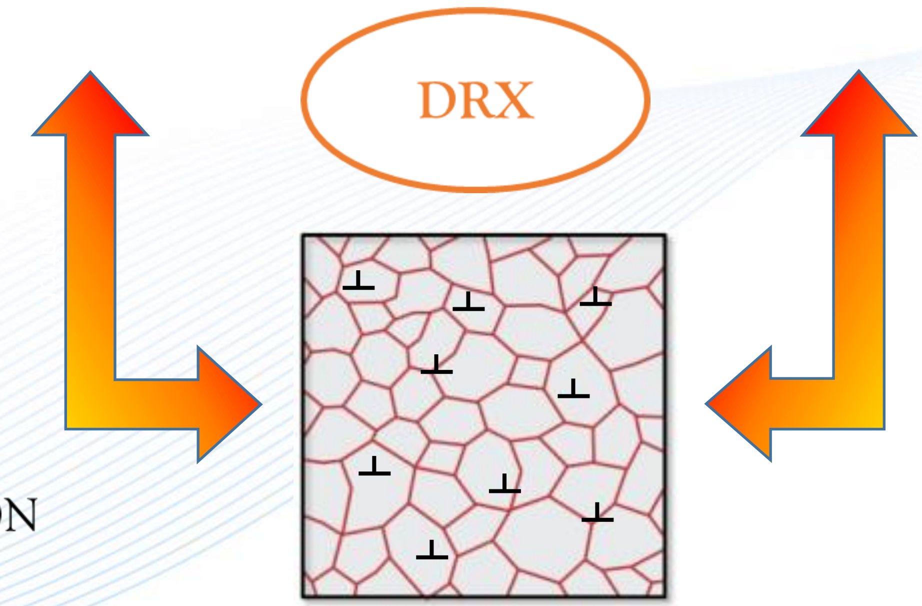

GRAIN BOUNDARY MIGRATION

DRX

- STRAIN HARDENING
- DYNAMIC RECOVERY
- NUCLEATION
- GRAIN BOUNDARY MIGRATION

Post-Dynamic Recrystallization (PDRX)

Microstructure after hot deformation

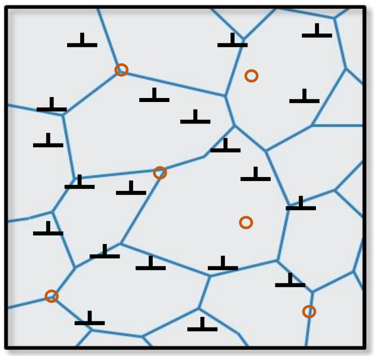

High T°

GRAIN BOUNDARY MIGRATION

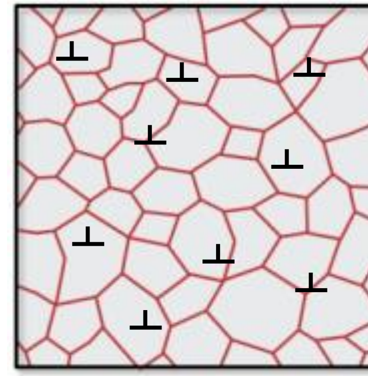

PDRX

High T°

STATIC RECOVERY + NUCLEATION

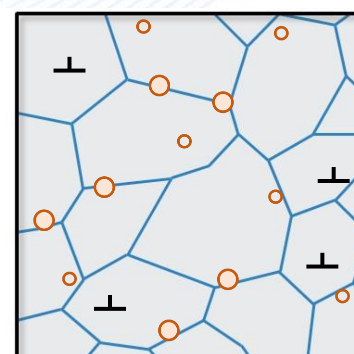

PDRX

- STATIC RECOVERY
- NUCLEATION
- GRAIN BOUNDARY MIGRATION

Context of the study

Hot forming

(www.sassda.co.za)

microstructure

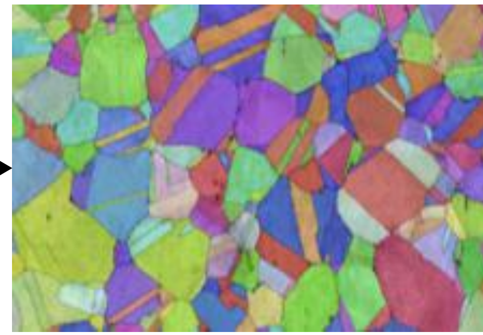

final properties

(Bobin et al., 2015)

Importance to predict, control and optimize microstructural evolutions by DRX and PDRX

Context of the study

Hot forming → **microstructure** → **final properties**

(www.sassda.co.za)

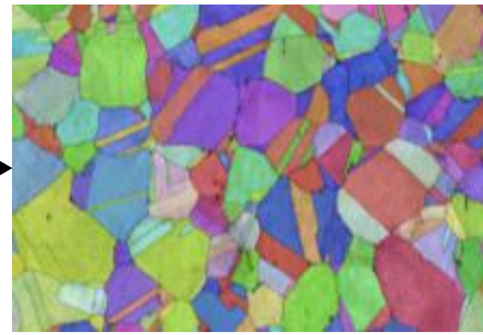

(Bobin et al., 2015)

Importance to predict, control and optimize microstructural evolutions by DRX and PDRX

➢ Simulations

Context of the study

Hot forming

(www.sassda.co.za)

microstructure

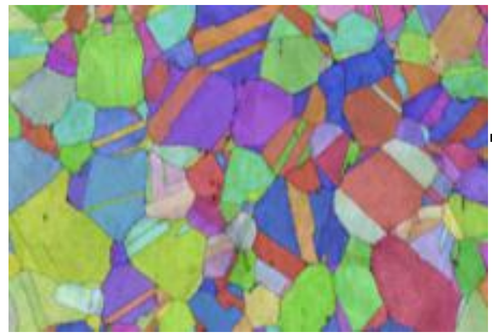

final properties

(Bobin et al., 2015)

Finite element simulation

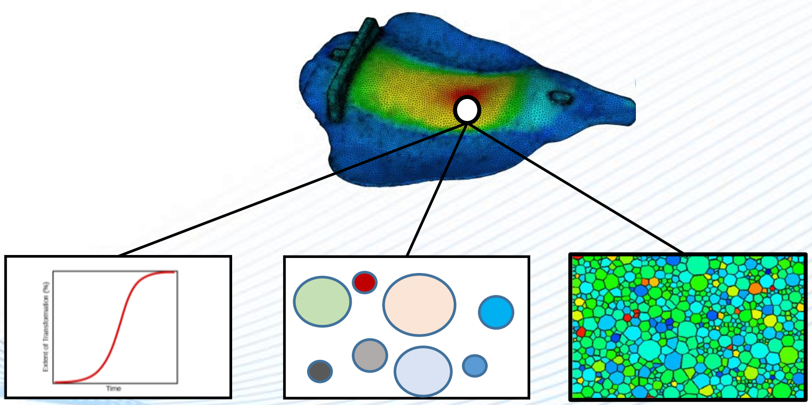

Phenomenological | Mean field | Full field

Finite element simulation

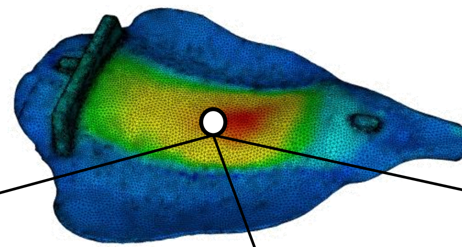

Phenomenological models

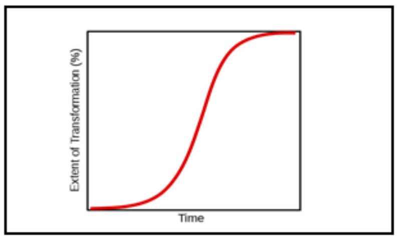

↗ Analytical laws (fast)

→ Averaged quantities

↘ Recalibration for each particular condition (T°, $\dot{\varepsilon}$)

↘ No description of the microstructure

Mean field models

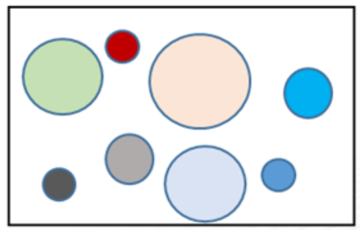

↗ Implicit description of the microstructure

↗ Versatile

↗ Analytical laws

→ Prediction of grain size distributions

→ Local mechanisms

→ Homogenized microstructure

Full field models

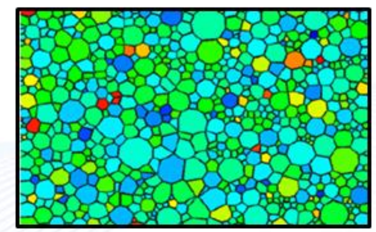

↗ Versatile

↗ Local mechanisms

↗ Explicit description of the microstructure

↘ Numerical costs

Finite element simulation

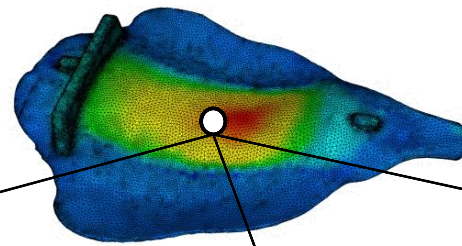

Phenomenological models

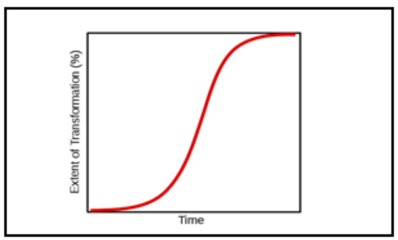

↗ Analytical laws (fast)

→ Averaged quantities

↘ Recalibration for each particular condition (T°, $\dot{\varepsilon}$)
↘ No description of the microstructure

Mean field models

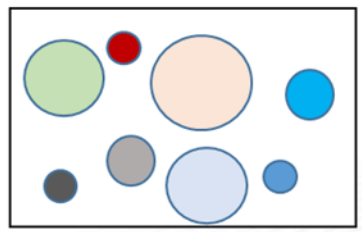

↗ Implicit description of the microstructure
↗ Versatile
↗ Analytical laws
→ Prediction of grain size distributions
→ Local mechanisms
→ Homogenized microstructure

Full field models

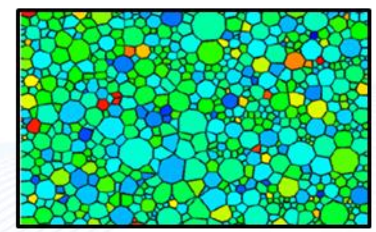

↗ Versatile
↗ Local mechanisms
↗ Explicit description of the microstructure

↘ Numerical costs

Full field modeling : The Level-Set method in a finite element framework

L. Maire, B. Scholtes, C. Moussa, N. Bozzolo, D. Pino Muñoz, A. Settefrati, M. Bernacki, Modeling of dynamic and post-dynamic recrystallization by coupling a full field approach to phenomenological laws, Materials & Design 133 (2017) 498–519.

➢ A Level-Set method in a finite element framework is considered in this work

The Level-Set method

Level-Set functions :

$$\begin{cases} \psi(x) = d(x,\Gamma), x \in \Omega, \\ \Gamma = \{x \in \Omega, \psi(x) = 0\} \end{cases}$$

(Merriman et al., 1994, Bernacki et al., 2008)

(Osher and Sethian, 1988)

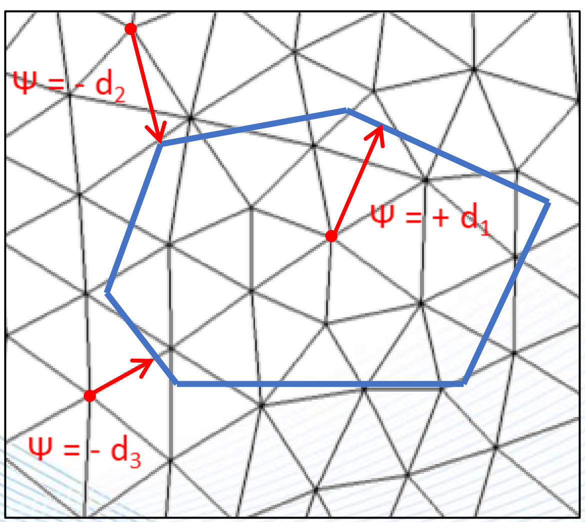

Generation of the initial microstructure

- Immersion of experimental micrographs
- Using a Voronoï tessellation
- Using a Laguerre-Voronoï tessellation

(Hitti et al., 2012, Fan et al., 2004)

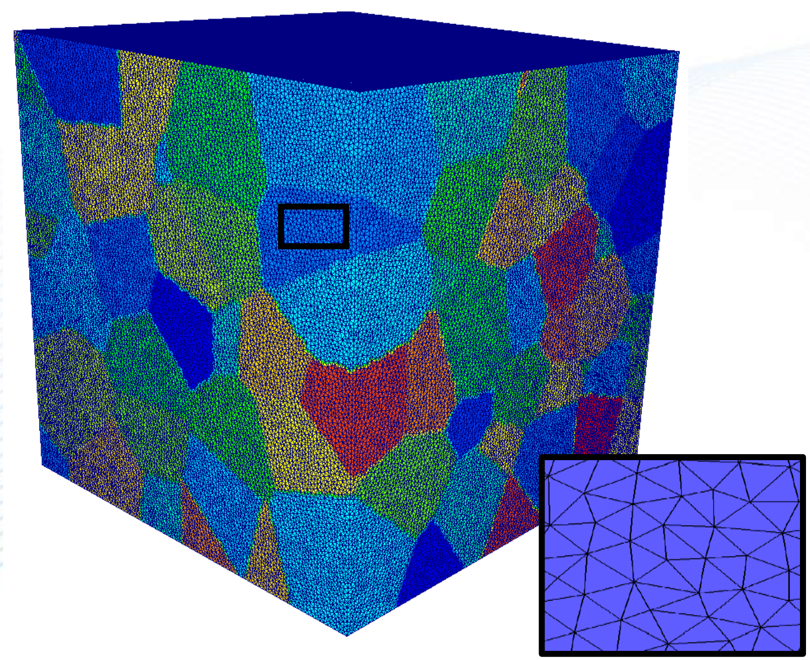

➢ The Level-Set method captures interfaces

Interfaces displacement

$$\begin{cases} \dfrac{\partial \psi_i(x,t)}{\partial t} + \vec{v}_i . \vec{\nabla} \psi_i(x,t) = 0 \\ \psi_i(t=0,x) = \psi_i^0(x) \end{cases}$$

$+$

Reinitialization of the Level-Set functions

$$||\nabla \psi_i|| = 1$$

Numerical tools to decrease computational costs

- Use of a recoloring schema with GLS functions

(PhD Scholtes 2013-2016, Scholtes et al. CMS 2015; Scholtes et al. CMS 2016)

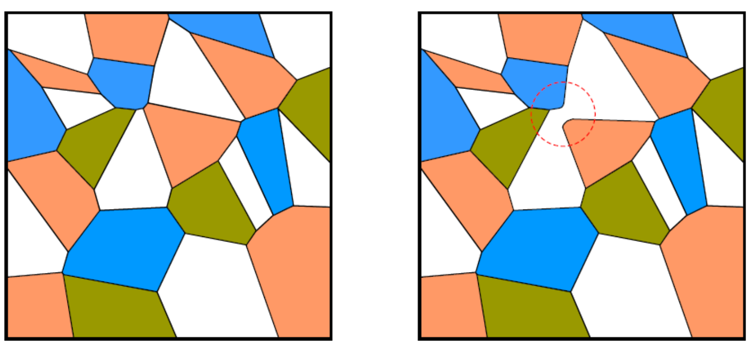

- Use of a direct reinitialization algorithm

(Shakoor & Scholtes, AMM 2015)

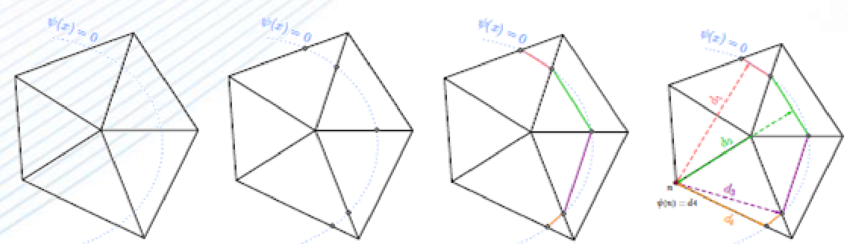

A new full field model for DRX and PDRX

L. Maire, B. Scholtes, C. Moussa, N. Bozzolo, D. Pino Muñoz, A. Settefrati, M. Bernacki, Modeling of dynamic and post-dynamic recrystallization by coupling a full field approach to phenomenological laws, Materials & Design 133 (2017) 498–519.

Dynamic Recrystallization (DRX)

Initial microstructure

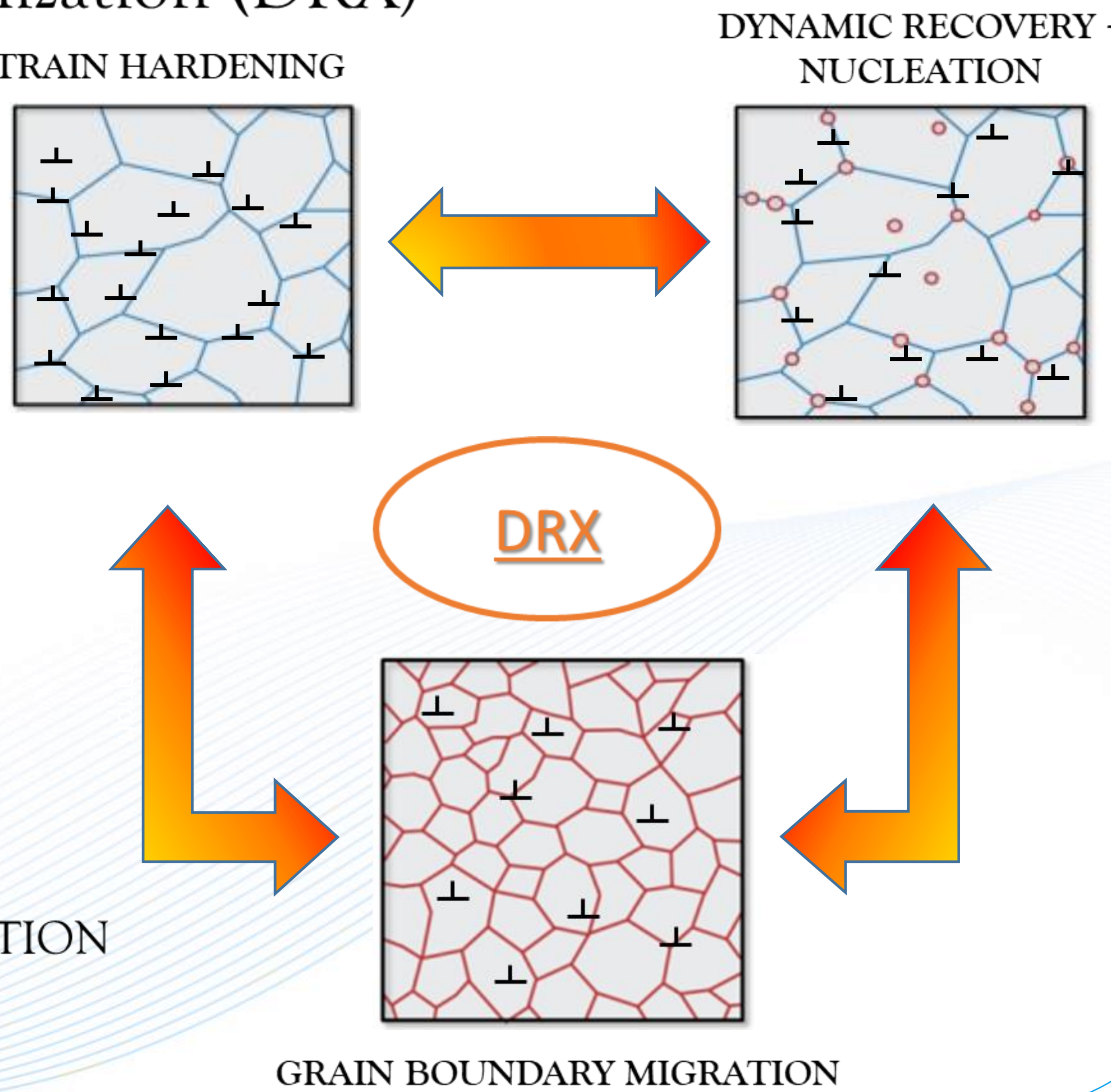

DRX

- STRAIN HARDENING
- DYNAMIC RECOVERY
- NUCLEATION
- GRAIN BOUNDARY MIGRATION

Mechanisms considered for **DRX**

Strain hardening/Recovery

(Yoshie et al., 1987)

$$\boxed{\frac{\partial \rho_i}{\partial \varepsilon} = K_1 - K_2 \rho_i}$$

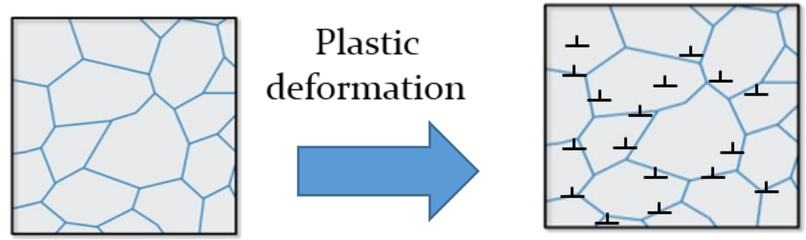

Nucleation

(Roberts et al., 1978)
(Beltran et al., 2015)
(Bailey & Hirsch, 1962)

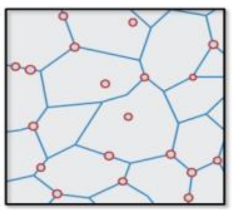

When/Where ?

$$\rho_{cr} = \left(\frac{20 K_1 \gamma_b \dot{\varepsilon}}{3 M_b \delta \tau^2}\right)^{1/3}.$$

$$\rho_{cr} = \left[\frac{-2\gamma_b \dot{\varepsilon}\dfrac{K_2}{M_b \delta \tau^2}}{\ln\left(1 - \dfrac{K_2}{K_1}\rho_{cr}\right)}\right]^{1/2}$$

Which size ?

$$\boxed{r_{cr} = \omega \frac{2\gamma_b}{\rho_{cr}\tau}}$$

How many ?

$$\boxed{\dot{V} = K_g \Phi \Delta t}$$

Boundary migration

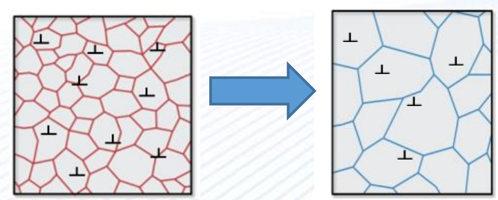

(Bernacki et al., 2011)

$$\begin{cases} \dfrac{\partial \psi_i(x,t)}{\partial t} - M_b \gamma_b \Delta \psi_i + \vec{v_i^e} . \nabla \psi_i = 0 \\ \psi_i(t=0,x) = \psi_i^0(x) \end{cases}$$

$$v_i^e = M_b[\delta\tau(\rho_j - \rho_i)]$$

Mechanisms considered for **PDRX**

Static Recovery

$$\frac{\partial \rho_i}{\partial t} = -K_s \rho_i$$

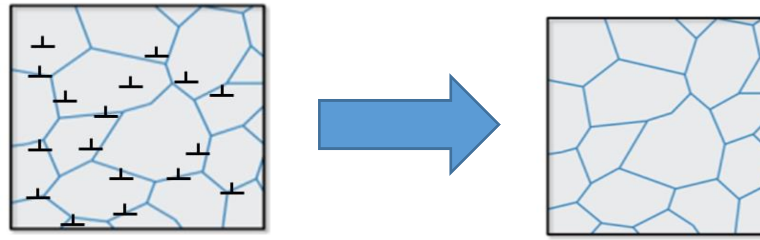

Nucleation

(Roberts et al., 1978)
(Beltran et al., 2015)
(Bailey & Hirsch, 1962)

ASSUMPTION

Which size ?

$$r_{cr} = \omega \frac{2\gamma_b}{\rho_{cr}\tau}$$

When/Where ?

$$\rho_{cr} = \left(\frac{20K_1\gamma_b\dot{\varepsilon}}{3M_b\delta\tau^2}\right)^{1/3}.$$

$$\rho_{cr} = \left[\frac{-2\gamma_b\dot{\varepsilon}\frac{K_2}{M_b\delta\tau^2}}{\ln\left(1-\frac{K_2}{K_1}\rho_{cr}\right)}\right]^{1/2}$$

How many ?

$$\dot{V} = K_g \Phi \Delta t$$

Boundary migration

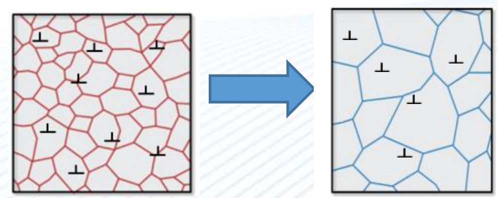

(Bernacki et al., 2011)

$$\begin{cases} \dfrac{\partial \psi_i(x,t)}{\partial t} - M_b\gamma_b\Delta\psi_i + \vec{v_i^e}.\nabla\psi_i = 0 \\ \psi_i(t=0,x) = \psi_i^0(x) \end{cases}$$

$$v_i^e = M_b[\delta\tau(\rho_j - \rho_i)]$$

Necklace nucleation in the considered full field framework

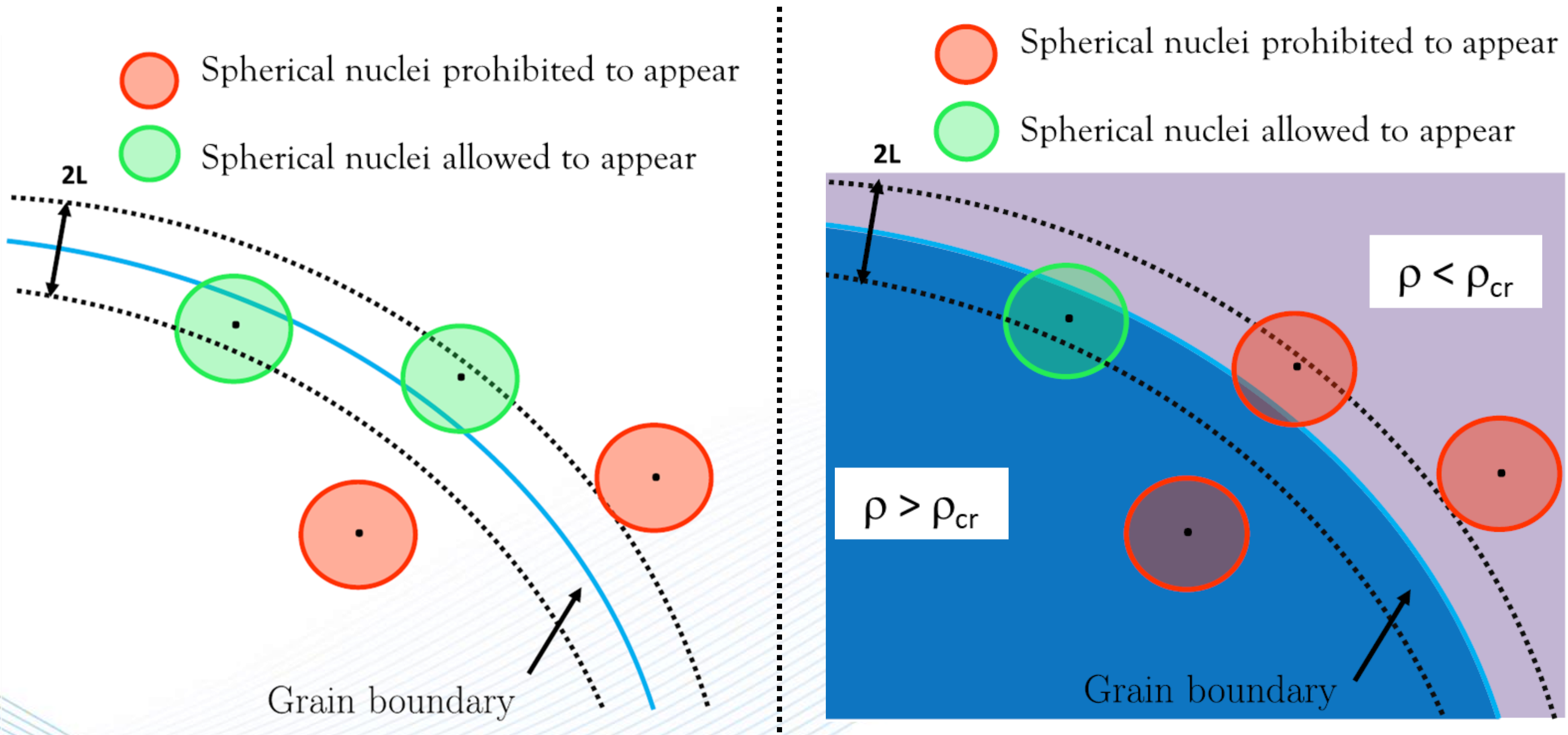

A multi-pass process simulated with the full field model

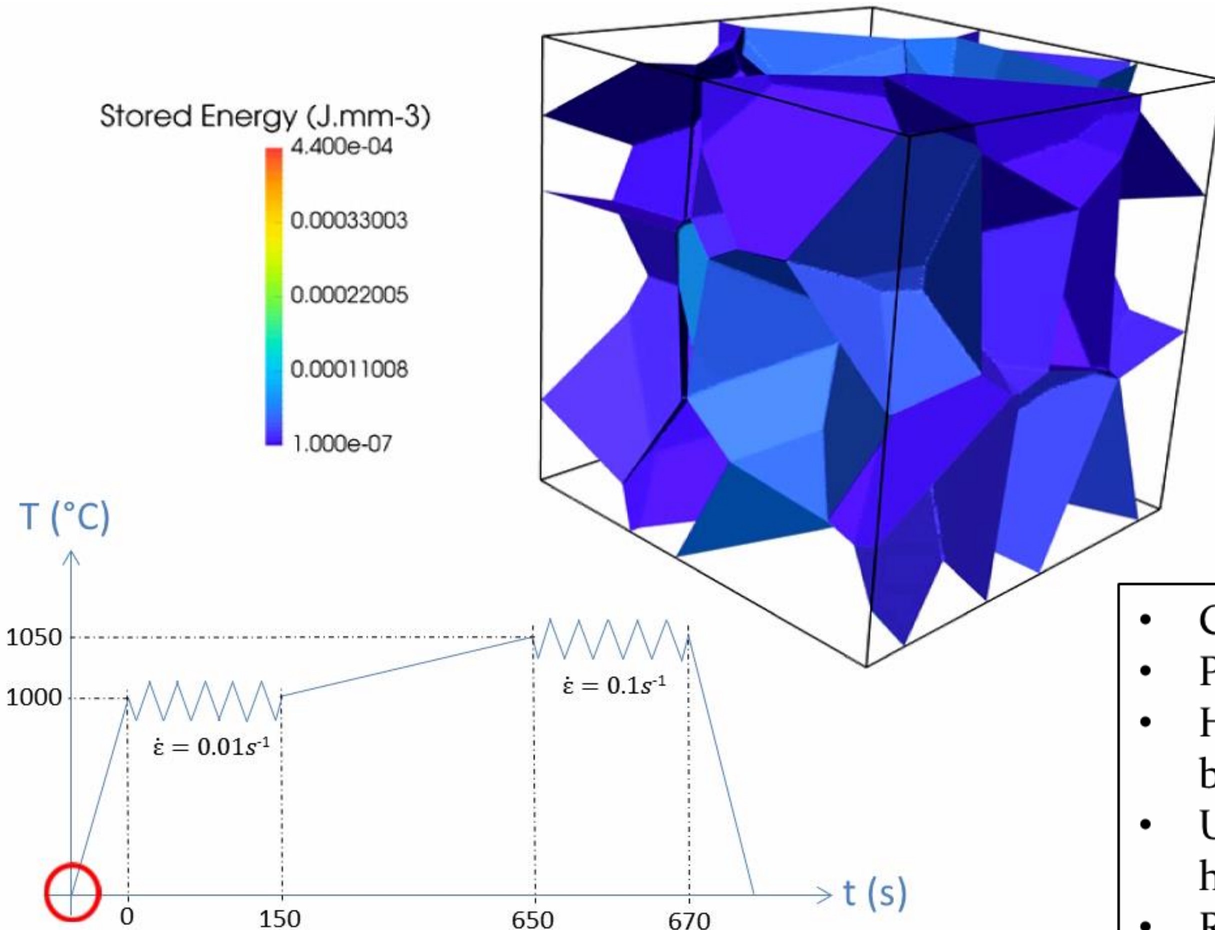

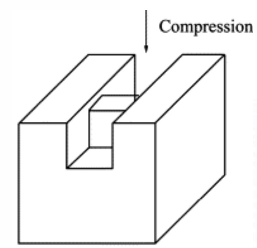

- Channel-die compression
- Parameters for a 304L steel
- Homogeneous values of grain boundary energy and mobility
- Unstructured, isotropic and homogeneous mesh
- Remeshing every 0.2 of deformation (best compromise)
- An initial number of 64 grains

Sensitivity study for integration in the DIGIMU software package

The sensitivity study identifies the ideal :

DRX

- initial number of grains
- safety factor for nuclei size
- deformation step
- mesh size

PDRX

- time step

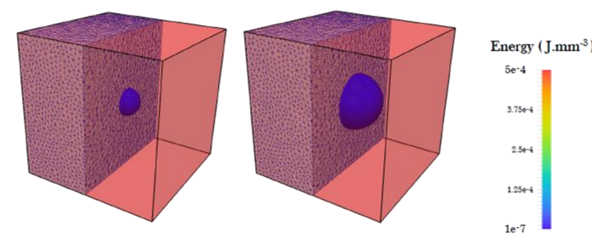

(a) $t = 0\mathrm{s}$ (b) $t = 50\mathrm{s}$

To converge in terms of :

- RX fraction
- mean grain size
- mean dislocation density
- grain size distributions
- dislocation density distributions

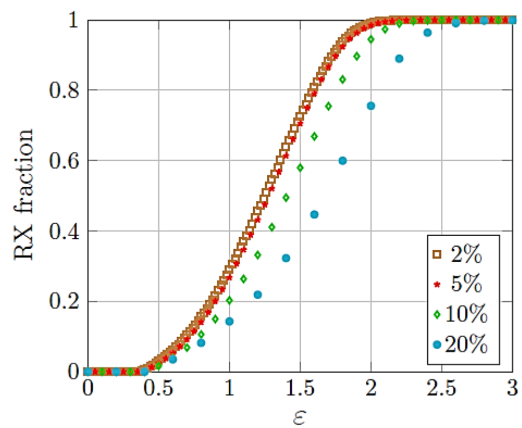

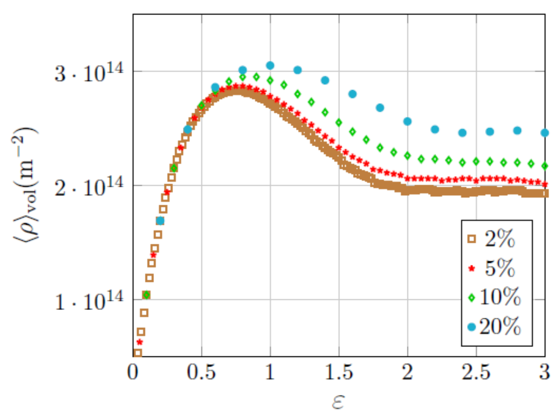

Simulation of DRX at T = 1273K and $\dot{\varepsilon}$=0.01s^{-1} during 200s

Before sensitivity study
10h on 3x24 procs

After sensitivity study
1h30 on 3x24 procs

A new topological approach for mean field modeling of DRX/PDRX

L. Maire, C. Moussa, N. Bozzolo, M. Bernacki, A new topological approach for the mean field modeling of dynamic recrystallization, Materials & Design 146 (2017) 194-207.

Finite element simulation

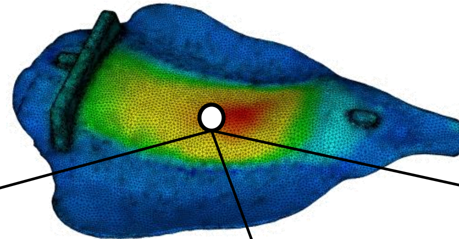

Phenomenological models

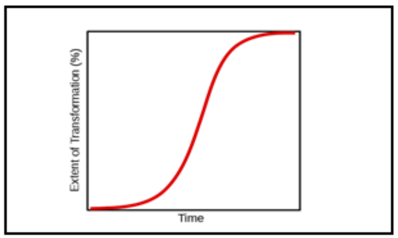

↗ Analytical laws (fast)

→ Averaged quantities

↘ Recalibration for each particular condition (T°, $\dot{\varepsilon}$)
↘ No description of the microstructure

Mean field models

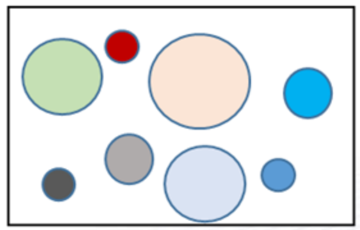

↗ Implicit description of the microstructure
↗ Versatile
↗ Analytical laws
→ Prediction of grain size distributions
→ Local mechanisms
→ Homogenized microstructure

Full field models

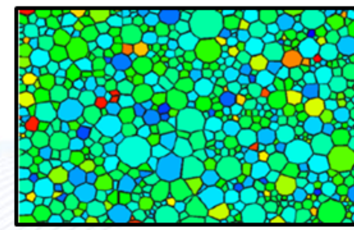

↗ Versatile
↗ Local mechanisms
↗ Explicit description of the microstructure

↘ Numerical costs

Mean field model (CEMEF)

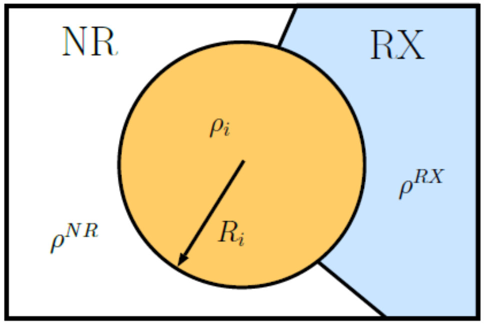

(Beltran et al., 2015)

Comparisons using same metallurgical laws with same model parameters

Full field model

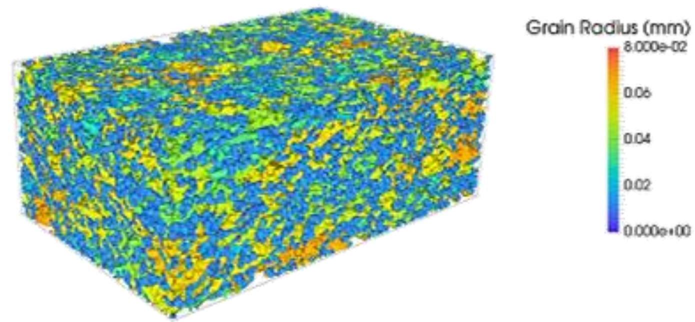

(Maire et al., 2017)

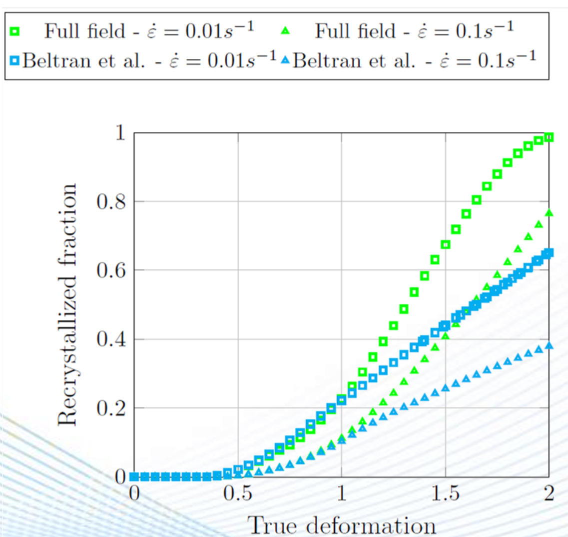

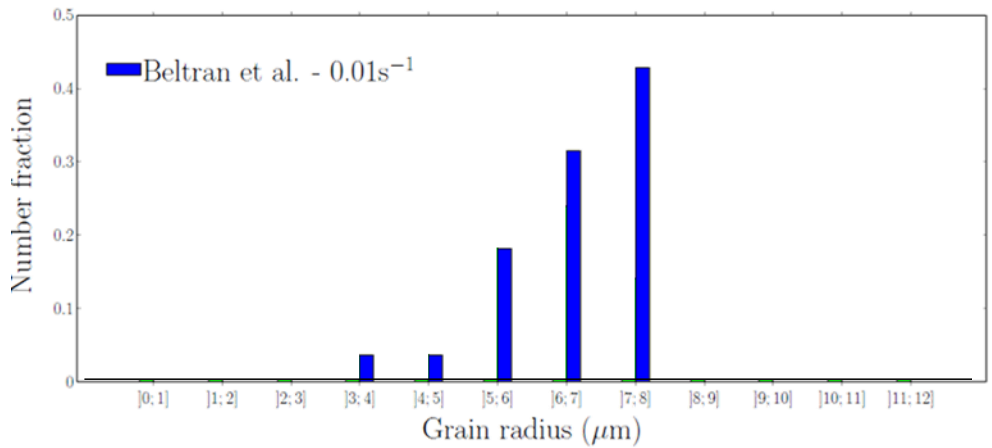

$\varepsilon = 1.5$

Limitation already discussed in many papers

(Beltran et al., 2015; Smagghe et al., 2016)

The *NHM* is based on two main improvements in terms of DRX mean field modeling :

I. The consideration of a particular neighborhood for each grain (topology)

II. The modeling of grain shape evolution during the dynamic process

The *NHM* is based on two main improvements in terms of DRX mean field modeling :

I. **The consideration of a particular neighborhood each grain (topology)**

II. The modeling of grain shape evolution during the dynamic process

The NHM vs Standard mean field models

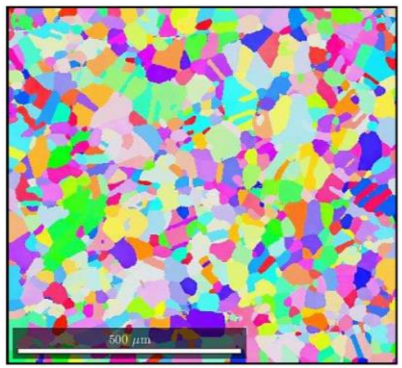

microstructure

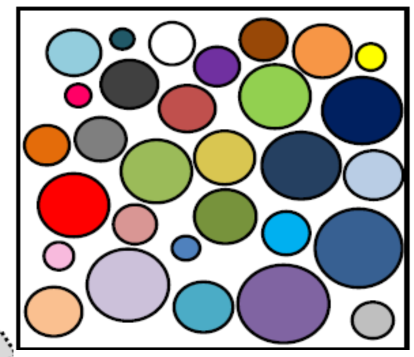

Mean field microstructure

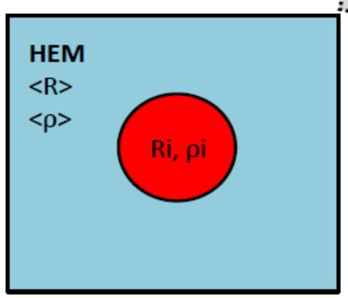

Former mean field models

(Hillert et al., 1965)
(Montheillet et al., 2009)
(Cram & Zurob, 2009)
(Beltran et al., 2015)

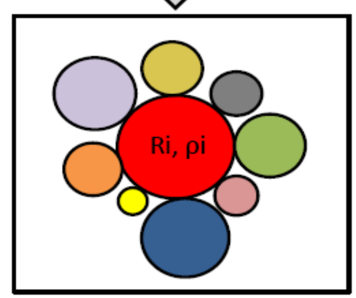

NHM

This new approach affects the grain boundary migration law

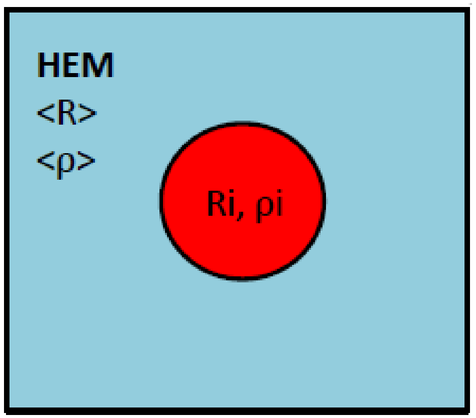

$$v_i = M_b\,[\delta\tau(\bar{\rho} - \rho_i) + \beta\gamma_b(\frac{1}{\bar{R}} - \frac{1}{R_i})]$$

$$\Delta V_i = v_i S_i \Delta t$$

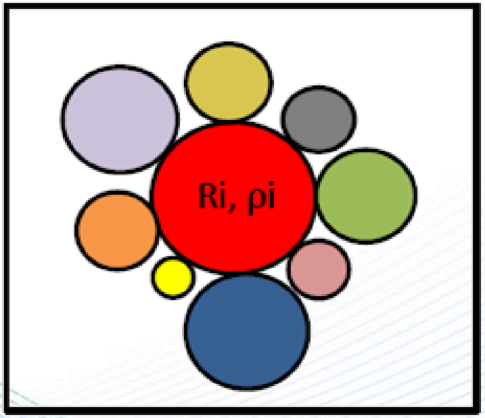

$$v_{ij} = M_b[\delta\tau(\rho_j - \rho_i) + \gamma_b(\frac{1}{R_j} - \frac{1}{R_i})]$$

$$\Delta V_{ij} = v_{ij}\, S_i\, \psi_{ij}\, \Delta t$$

Surface fraction in contact between *i* and *j*

How to choose the number of neighbors for each grain ?

- Some laws from literature predict the number of neighbors of a grain depending on its size, within a steady-state or quasi steady-state regime

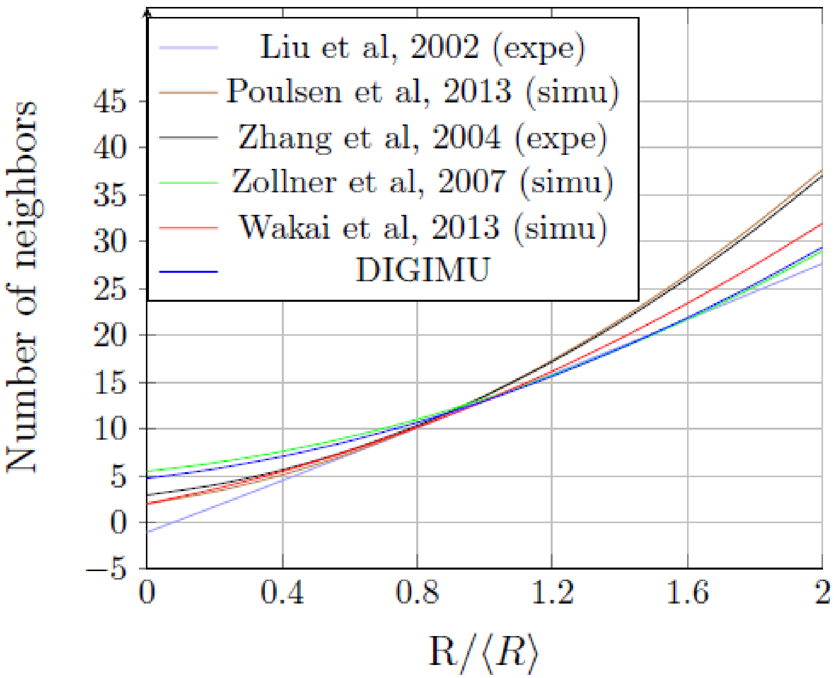

Validation with DIGIMU

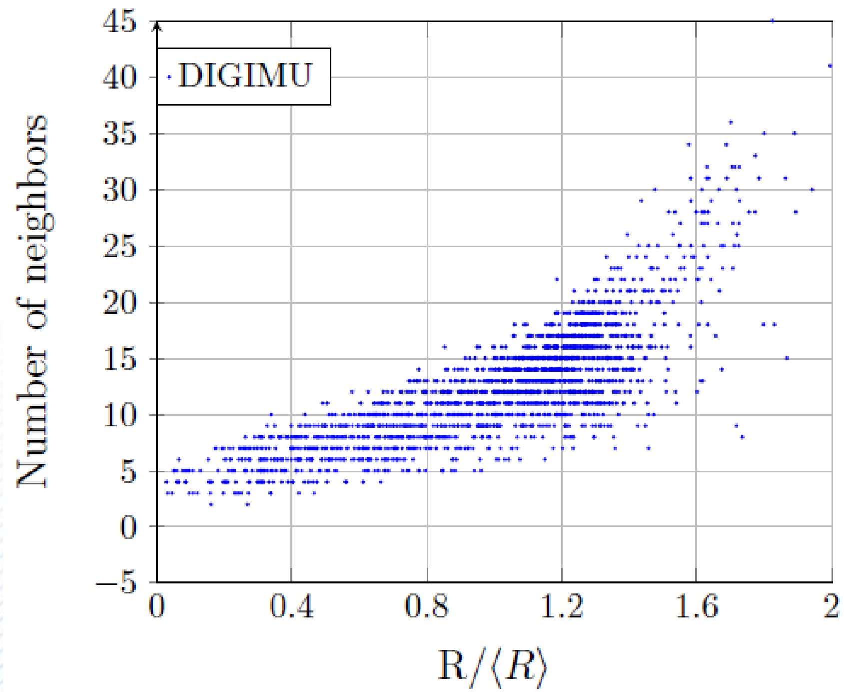

$$N_{neigh} = 4.06\omega^2 + 4.22\,\omega + 4.71$$
$$\text{with } \omega = R/\langle R \rangle$$

RESTRICTED

Number of neighbors occupying θ is subdivided into two families

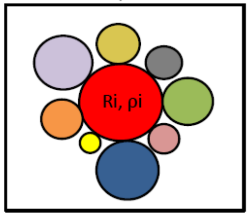

θ_1 : nuclei

θ_2 : Number of other RX grains

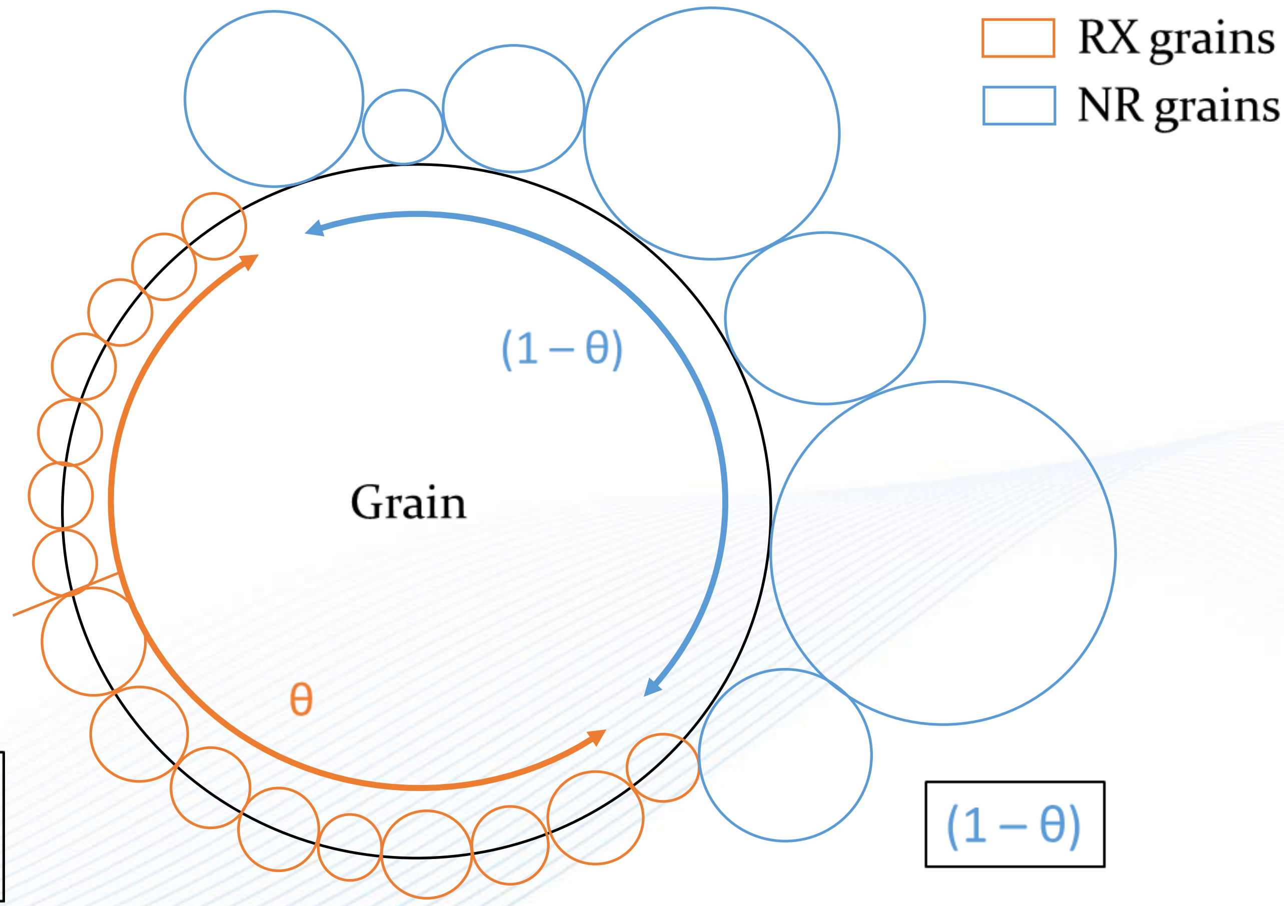

(1 – θ)

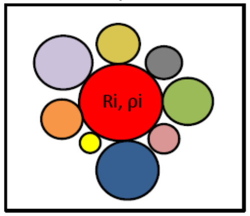

Number of neighbors occupying θ is subdivided into two families

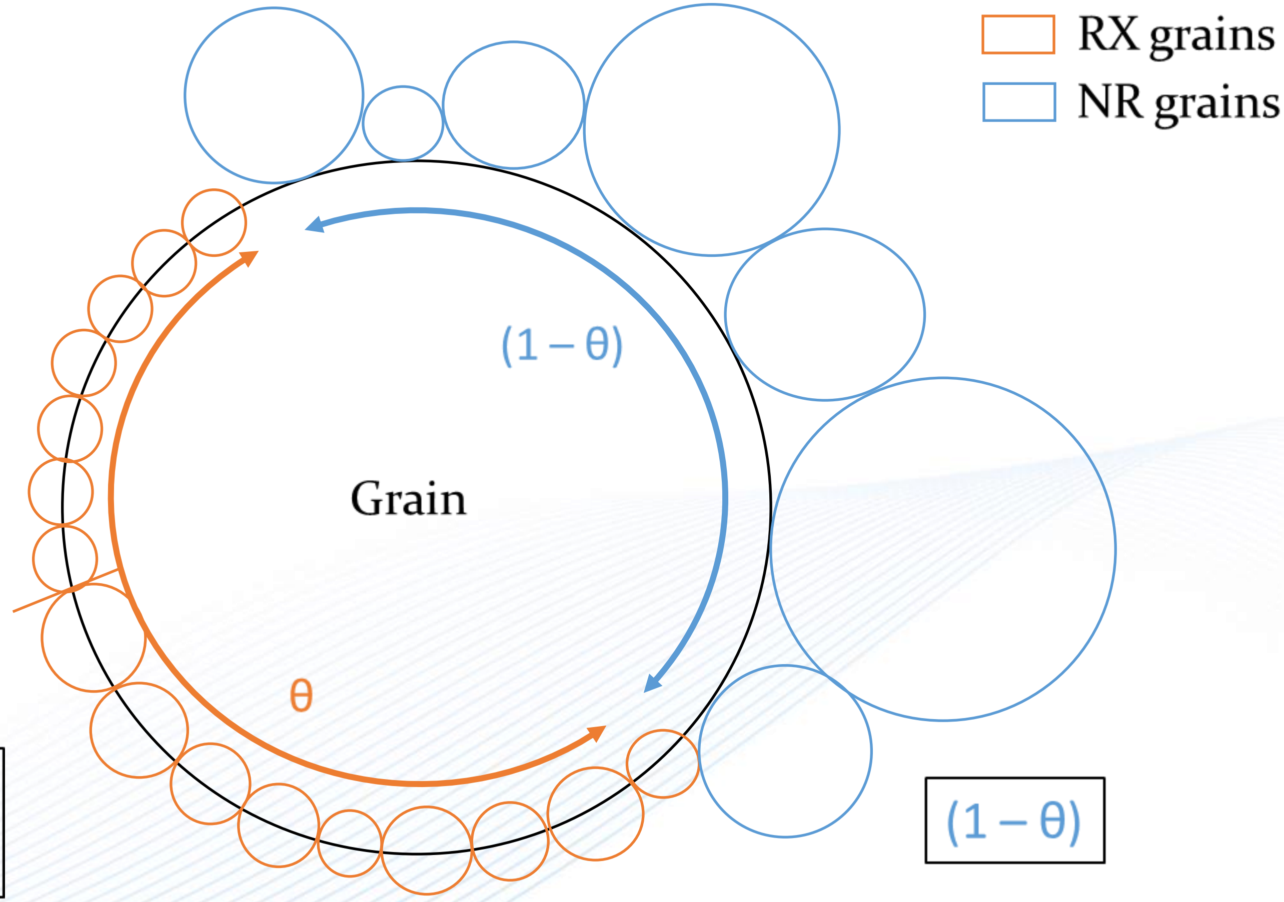

θ_1 : nuclei

- Known at any time increment

θ_2 : Number of other RX grains

- Known at any time increment

RESTRICTED

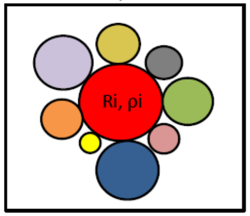

Number of neighbors occupying θ is subdivided into two families

θ_1 : nuclei

- Known at any time increment

θ_2 : Number of other RX grains

- Known at any time increment

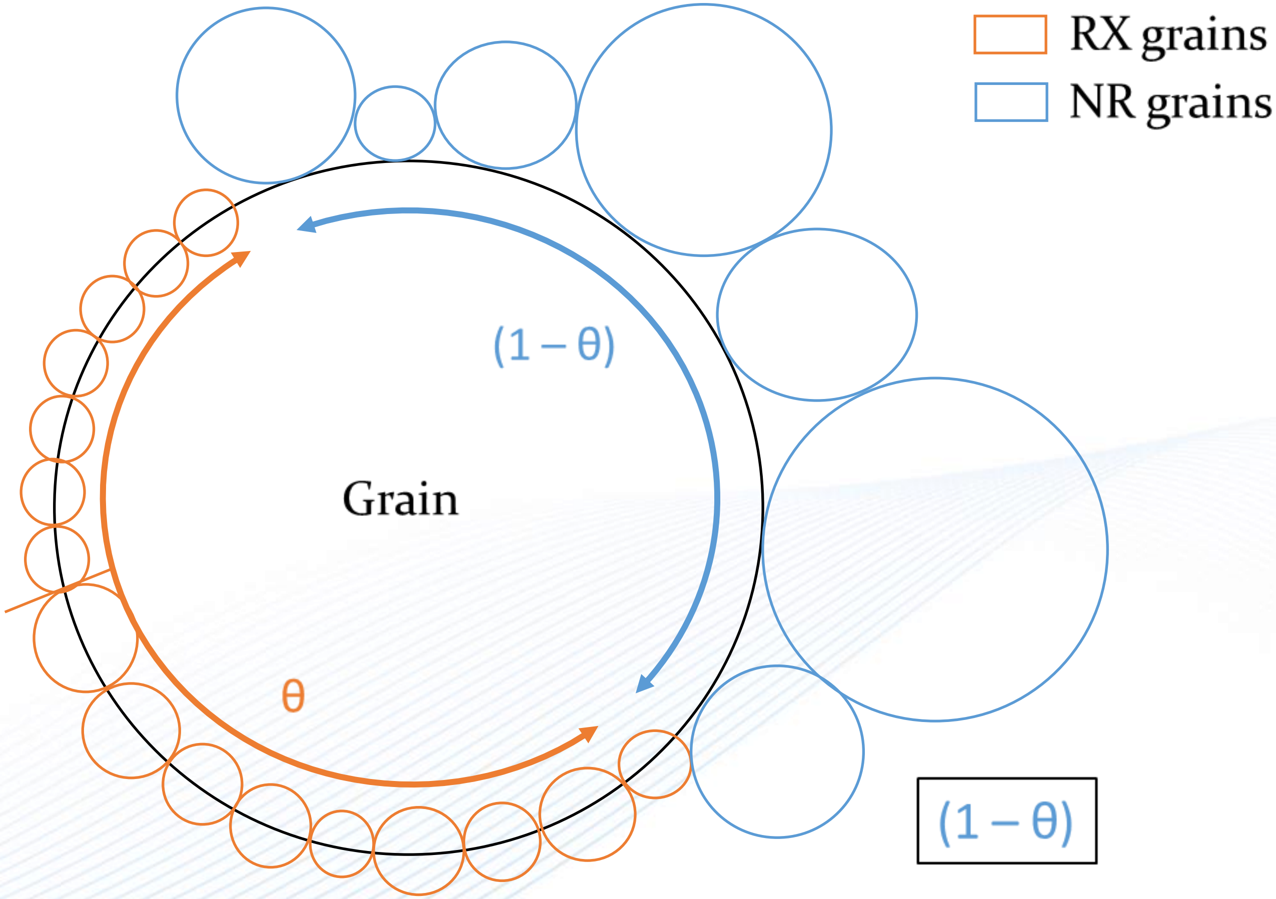

$$N_{neigh} = (4.06\omega^2 + 4.22\,\omega + 4.71)(1-\theta)$$
$$\text{with } \omega = R/\langle R_{NR}\rangle$$

The *NHM* is based on two main improvements in terms of mean field modeling :

I. The consideration of a particular neighborhood for each grain

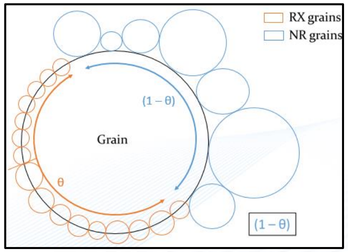

II. The modeling of the grain shape evolution

Standard Mean field models

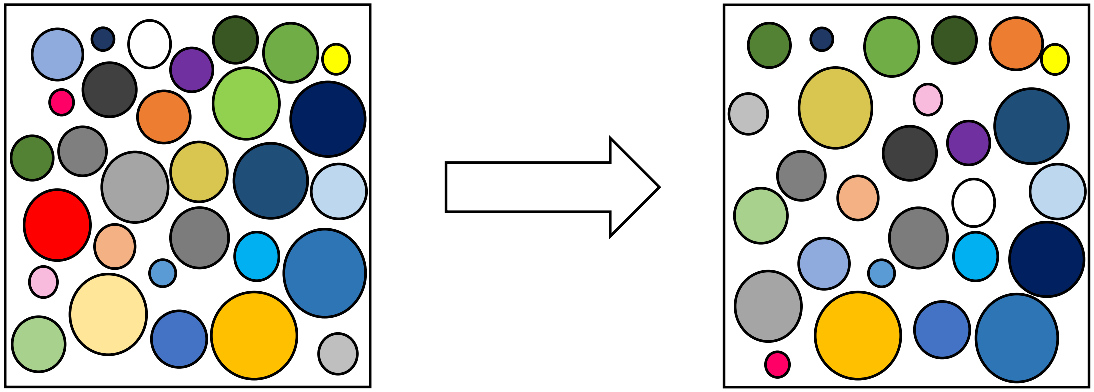

Grains remain spherical in MF models

Real microstructure

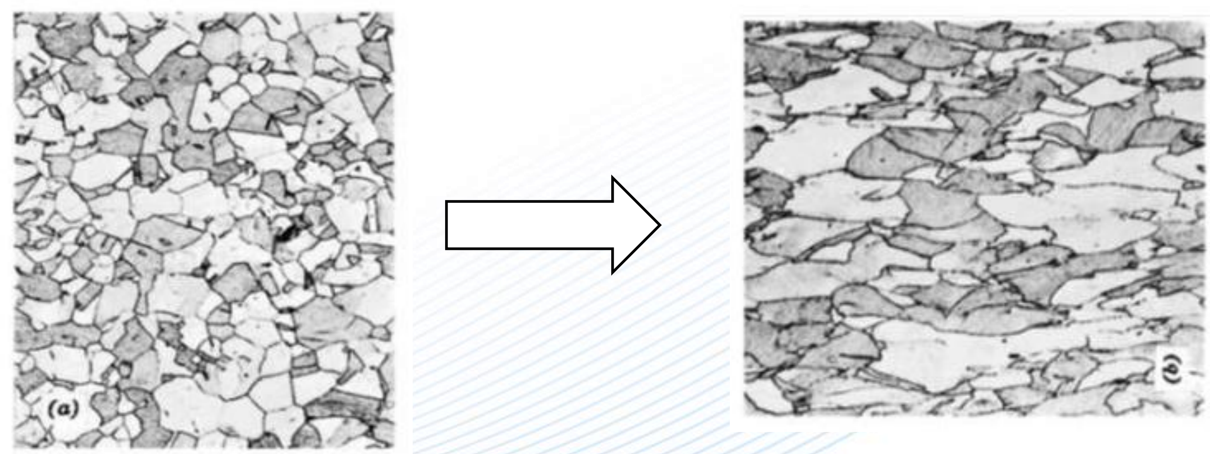

Grain shape evolves in real microstructure

(Source: Bergström, 2015)

RESTRICTED

Does the grain shape evolution influence results ?

By considering deformation

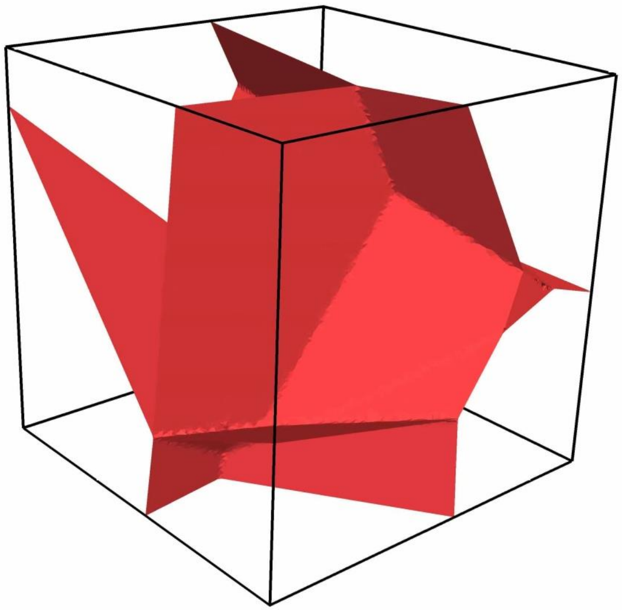

Without considering deformation

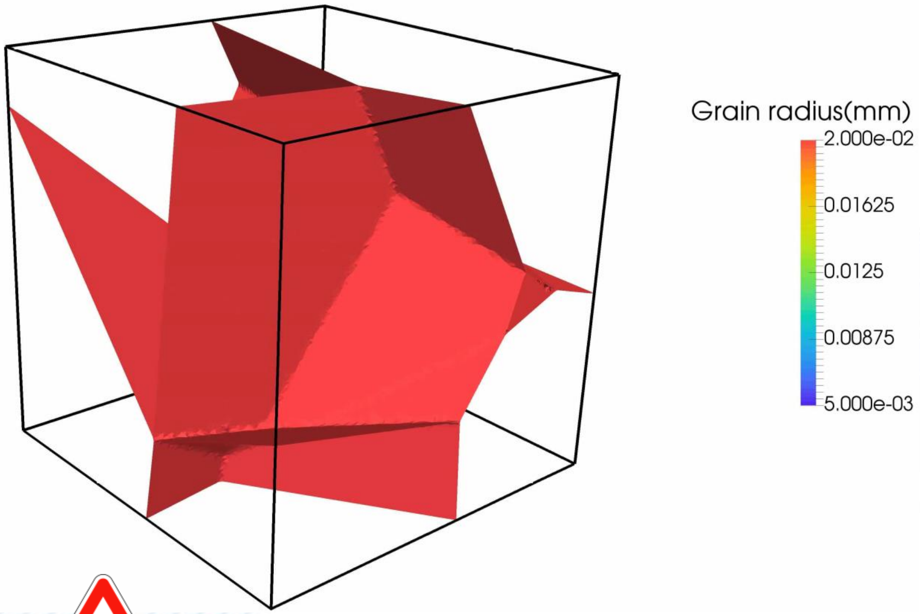

This case has no physical sense

RESTRICTED

Does the grain shape evolution influence results ?

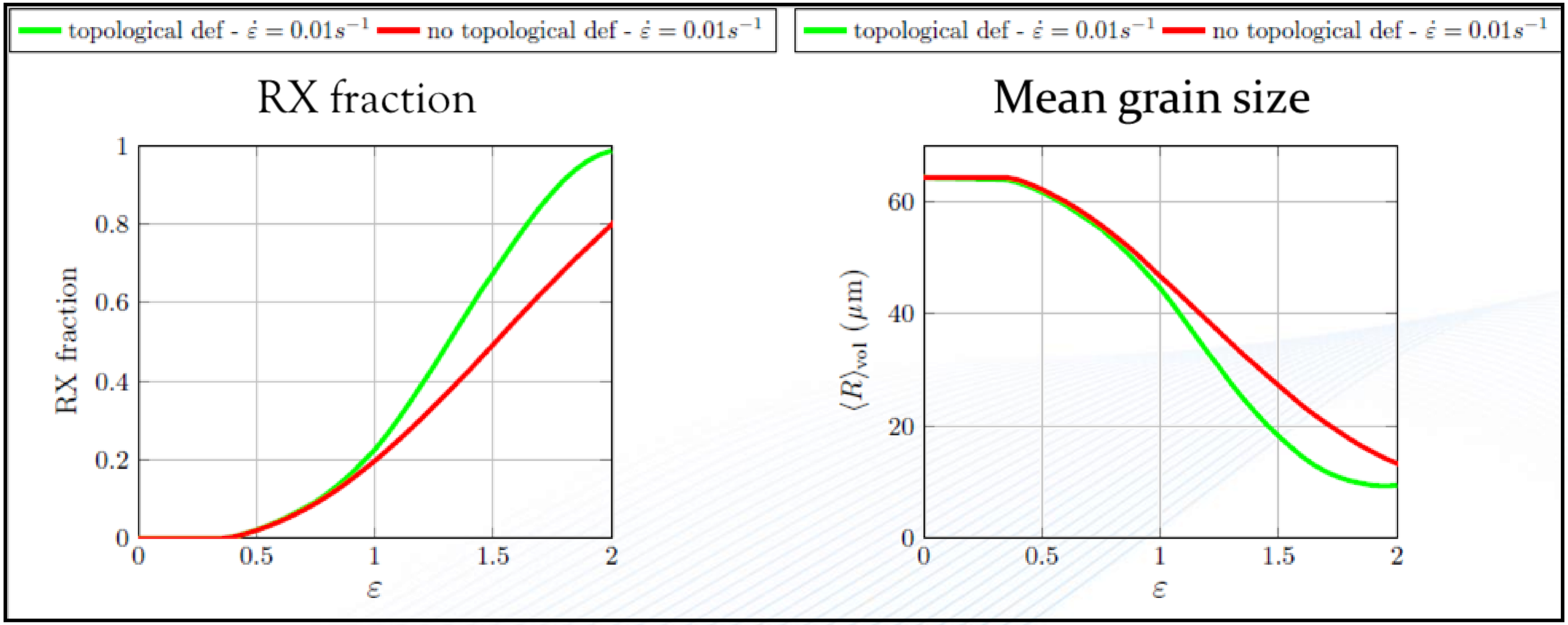

- Kinetics are faster in the physical case since grain boundary surface increases during deformation, increasing nucleation

How to consider grain shape evolution in the NHM ?

t_0

$\dot{\varepsilon}_{zz} = -0.01 s^{-1}$

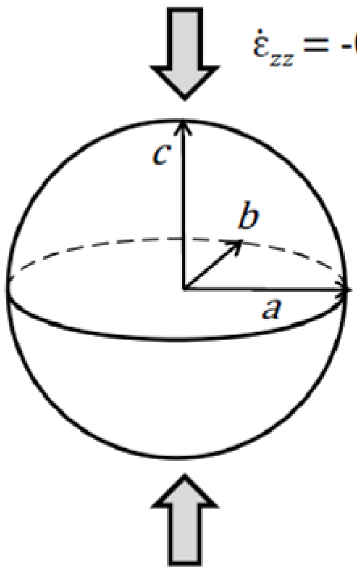

$(\alpha_1, \alpha_2, \alpha_3) = (1, 1, 1)$

$$\begin{cases} a = \alpha_1 R = R \\ b = \alpha_2 R = R \\ c = \alpha_3 R = R \end{cases}$$

Series of small time steps

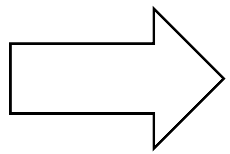

$$\alpha_1^{(t+\Delta t)} = \alpha_1^t + \dot{\varepsilon}_{xx}\Delta t,$$
$$\alpha_2^{(t+\Delta t)} = \alpha_2^t + \dot{\varepsilon}_{yy}\Delta t,$$
$$\alpha_3^{(t+\Delta t)} = \alpha_3^t + \dot{\varepsilon}_{zz}\Delta t,$$

$$M = \begin{bmatrix} \dot{\varepsilon}_{xx} & 0 & 0 \\ 0 & \dot{\varepsilon}_{yy} & 0 \\ 0 & 0 & \dot{\varepsilon}_{zz} \end{bmatrix}$$

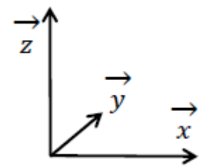

t_0 +20s

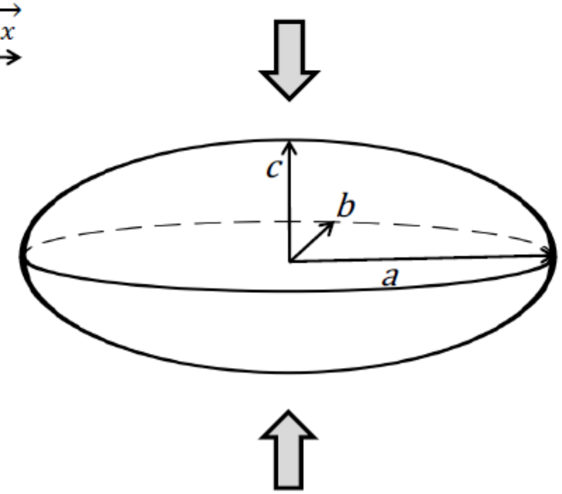

$(\alpha_1, \alpha_2, \alpha_3) = (1.105, 1.105, 0.82)$

$$\begin{cases} a = 1.105R \\ b = 1.105R \\ c = 0.818R \end{cases}$$

Final consideration of the neighborhood and the grain shape evolution :

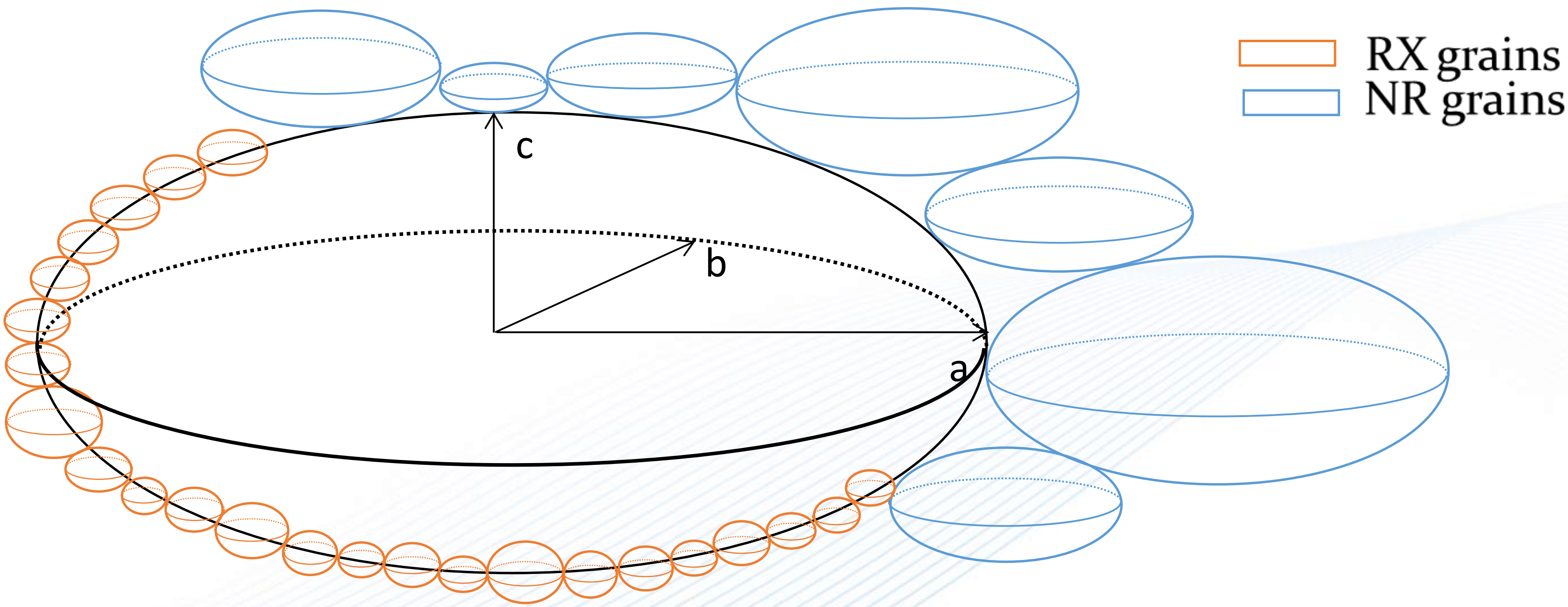

RESULTS USING THE NHM
In terms of :

1. RX Fraction and mean grain size
2. Grain size distributions

RESTRICTED

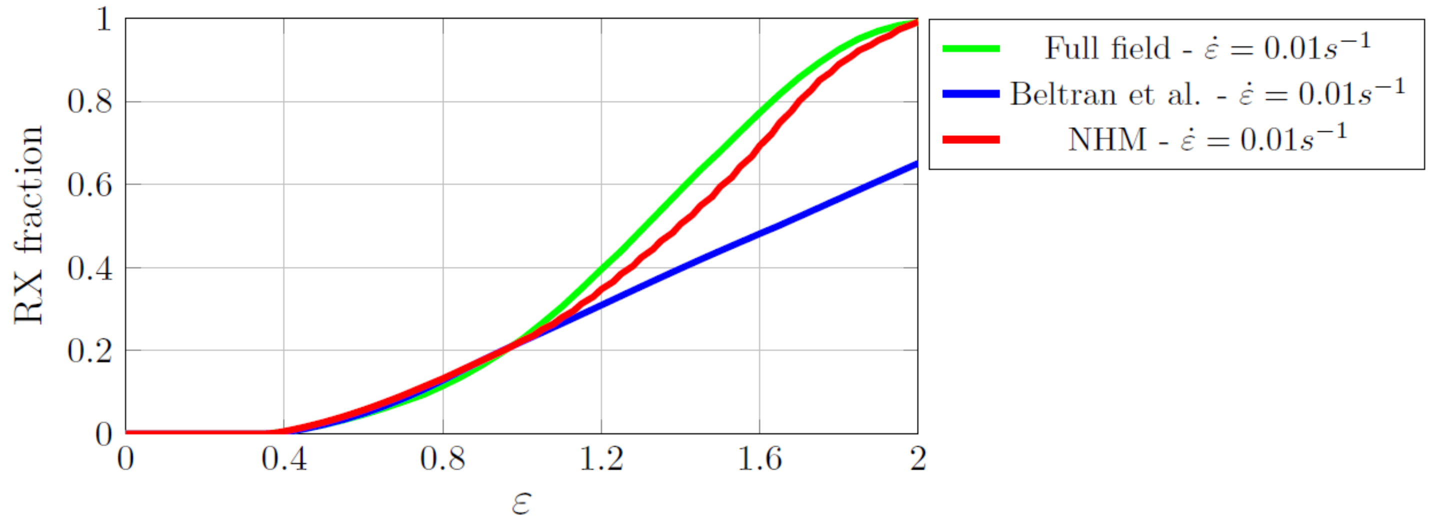
RX fraction
0
0.2
0.4
0.6
0.8
1
0
0.4
0.8
1.2
1.6
2
ε
Full field - $\dot{\varepsilon} = 0.01s^{-1}$
Beltran et al. - $\dot{\varepsilon} = 0.01s^{-1}$
NHM - $\dot{\varepsilon} = 0.01s^{-1}$

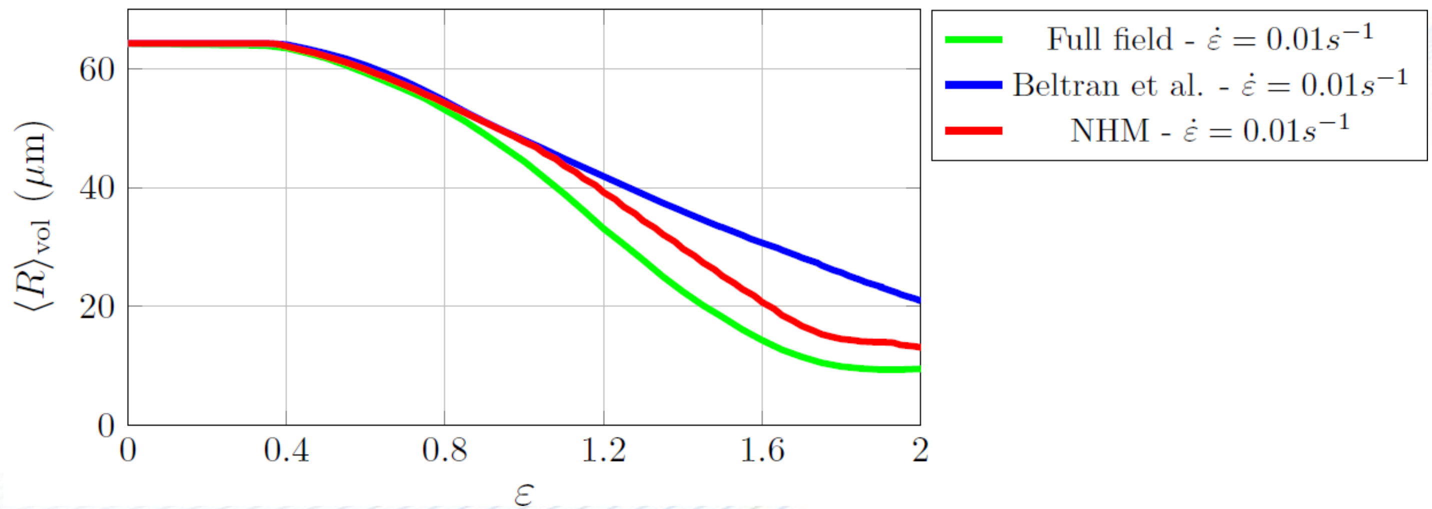
$\langle R \rangle_{\mathrm{vol}}$ (μm)
0
20
40
60
0
0.4
0.8
1.2
1.6
2
ε
Full field - $\dot{\varepsilon} = 0.01s^{-1}$
Beltran et al. - $\dot{\varepsilon} = 0.01s^{-1}$
NHM - $\dot{\varepsilon} = 0.01s^{-1}$

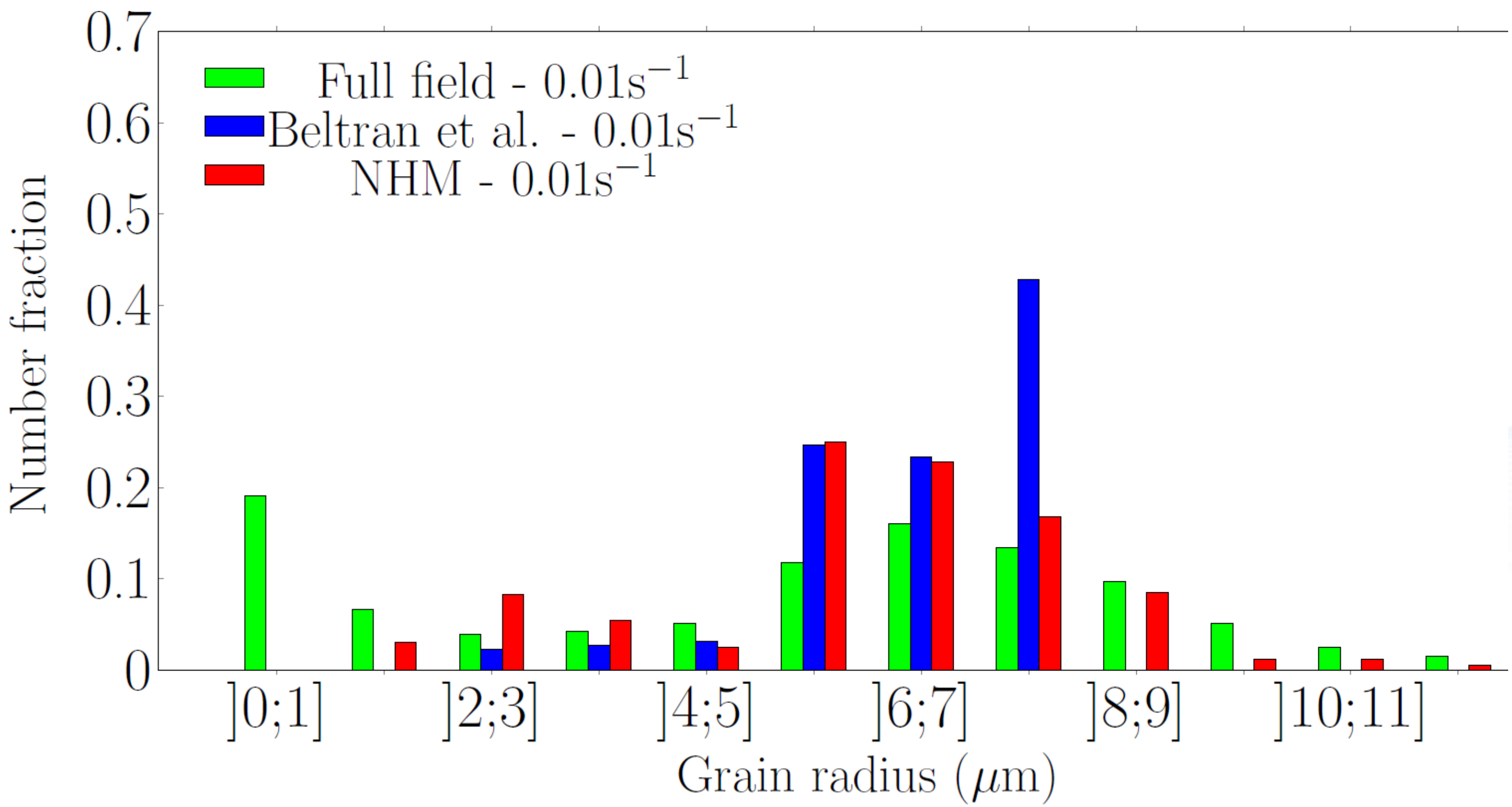

$$\varepsilon = 2$$

First integration of NHM into a finite element software

(J. Barlier from Transvalor S.A.)

Compression of a cylindrical sample

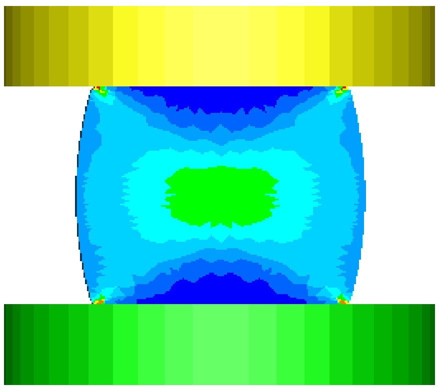

Sensors record the thermomechanical paths

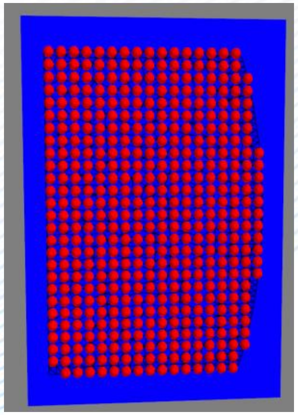

Prediction of microstructural quantities

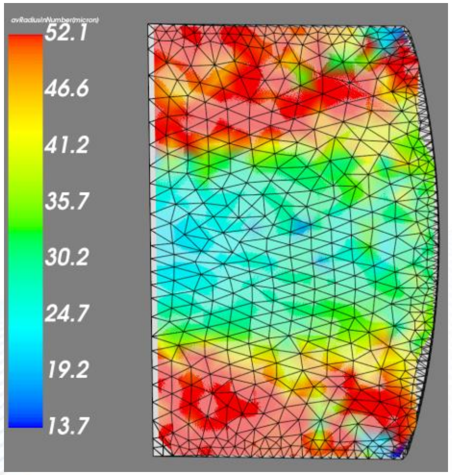

Experimental testings on 304L : Calibration and validation within the DRX regime

Compression test setup

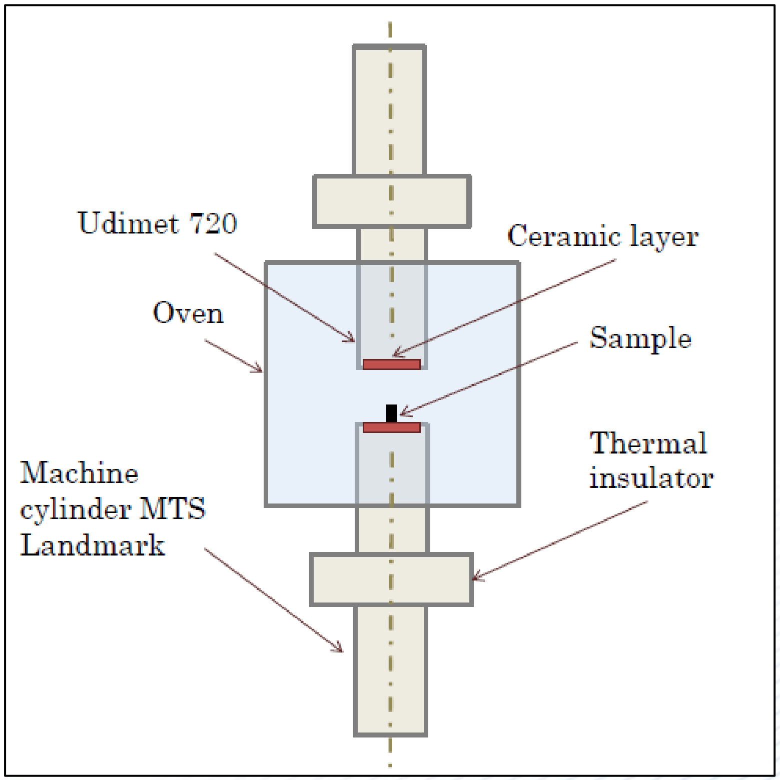

Thermomechanical conditions

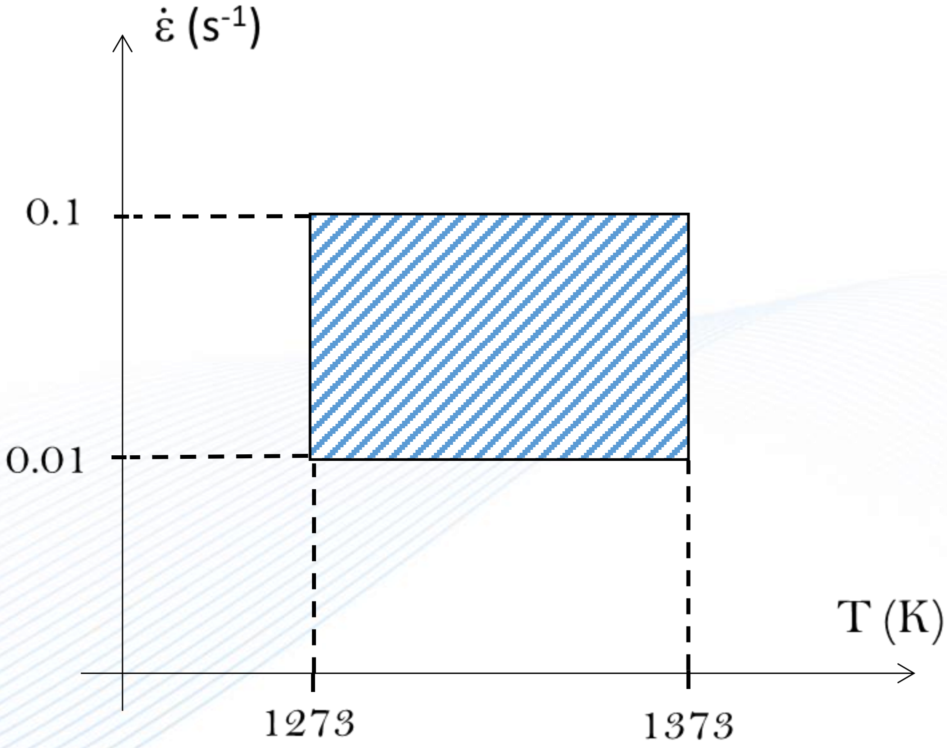

4 model parameters to be identified :

Hardening/Recovery

$$\frac{\partial \rho}{\partial \varepsilon} = K_1 - K_2 \rho$$

Identified on stress-strain curves before DRX initiates

Nucleation

$$\dot{V} = K_g S_b \Delta t$$

Grain boundary migration

$$v_{ij} = M\,[\delta\tau(\rho_j - \rho_i) + \gamma(\frac{1}{R_j} - \frac{1}{R_i})]$$

- Stress-strain curves required to identify K_1 and K_2

Effect of strain rate

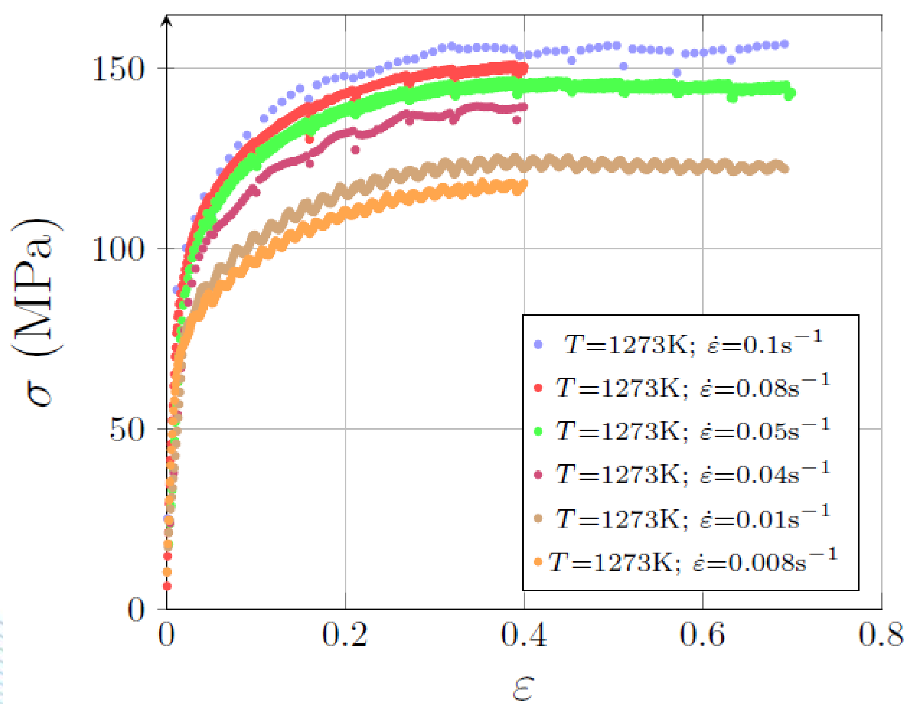

Effect of temperature

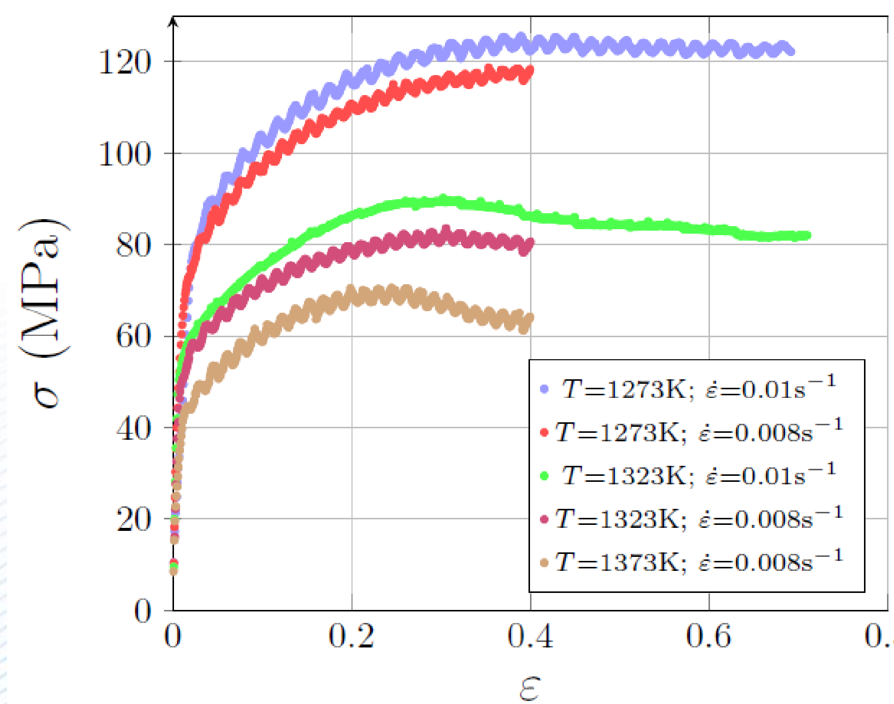

$$\frac{\partial \rho}{\partial \varepsilon} = K_1 - K_2 \rho$$

Identification of K1 and K2 based on stress-strain curves :

1. Method of Jonas et al. (2009) to get first approximations of K_1 and K_2

2. Inverse analysis on stress-strain curves using the Excel software. The portion of the curve considered is between yield stress and initiation of nucleation (about 80% of peak strain)

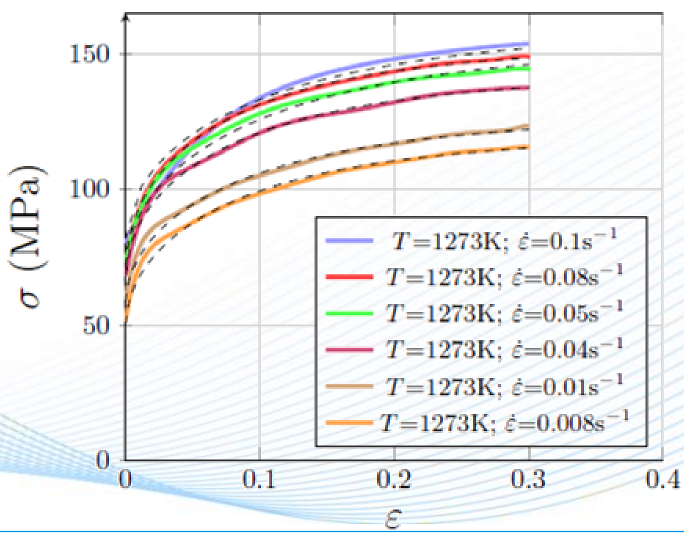

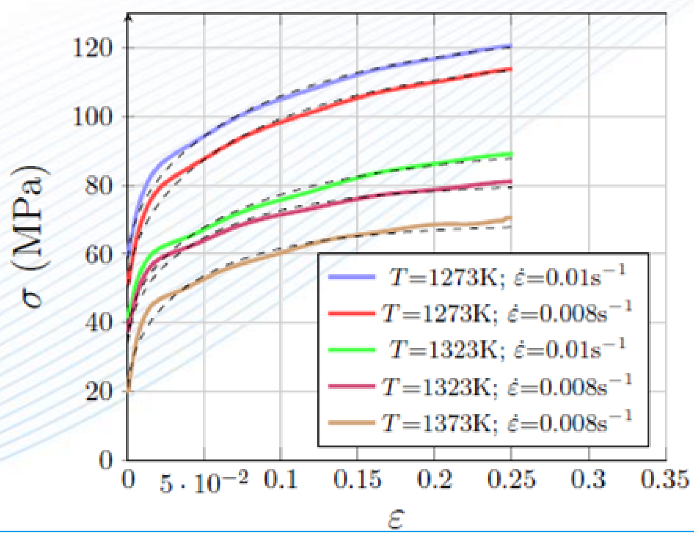

$$\frac{\partial \rho}{\partial \varepsilon} = K_1 - K_2 \rho$$

$$Z = \dot{\varepsilon} \exp\left(\frac{Q_{\mathrm{def}}}{RT}\right)$$

(Zener & Hollomon, 1944)

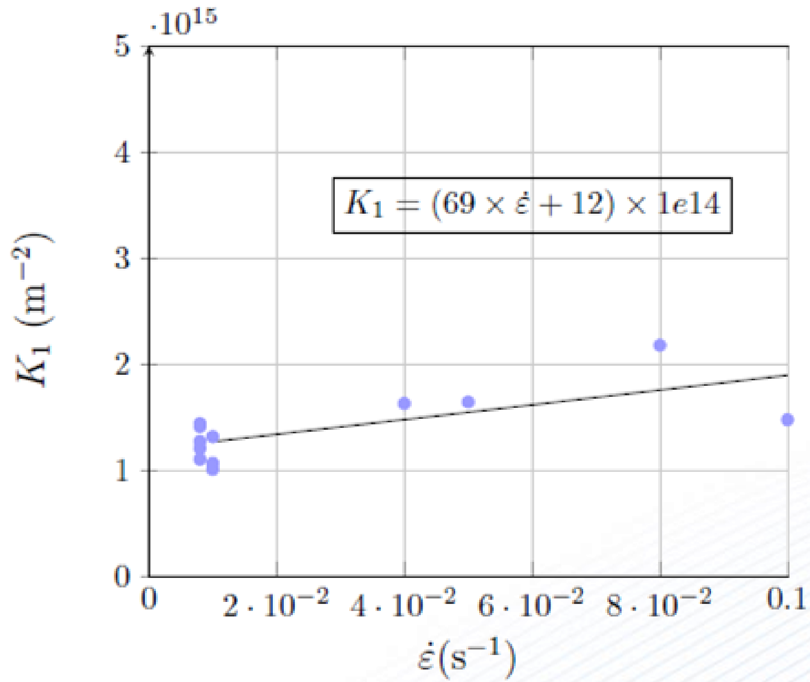

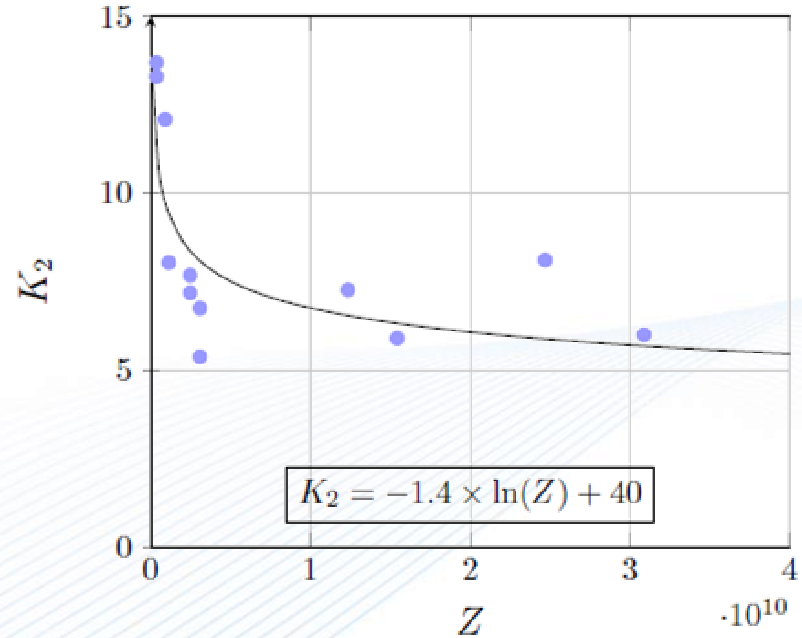

- Hardening is only dependent on strain rate and increases with it.
- Dynamic recovery decreases with strain rate and increases with temperature.
- Both parameter trends are in accordance with literature.

4 model parameters to be identified :

Hardening/Recovery

$$\frac{\partial \rho}{\partial \varepsilon} = K_1 - K_2 \rho$$

Identified on stress-strain curves before DRX initiates

Nucleation

$$\dot{V} = K_g S_b \Delta t$$

Grain boundary migration

$$v_{ij} = M \left[\delta\tau(\rho_j - \rho_i) + \gamma\left(\frac{1}{R_j} - \frac{1}{R_i}\right)\right]$$

Identified from microstructure investigations

RESTRICTED

RX fractions obtained from different samples after compression

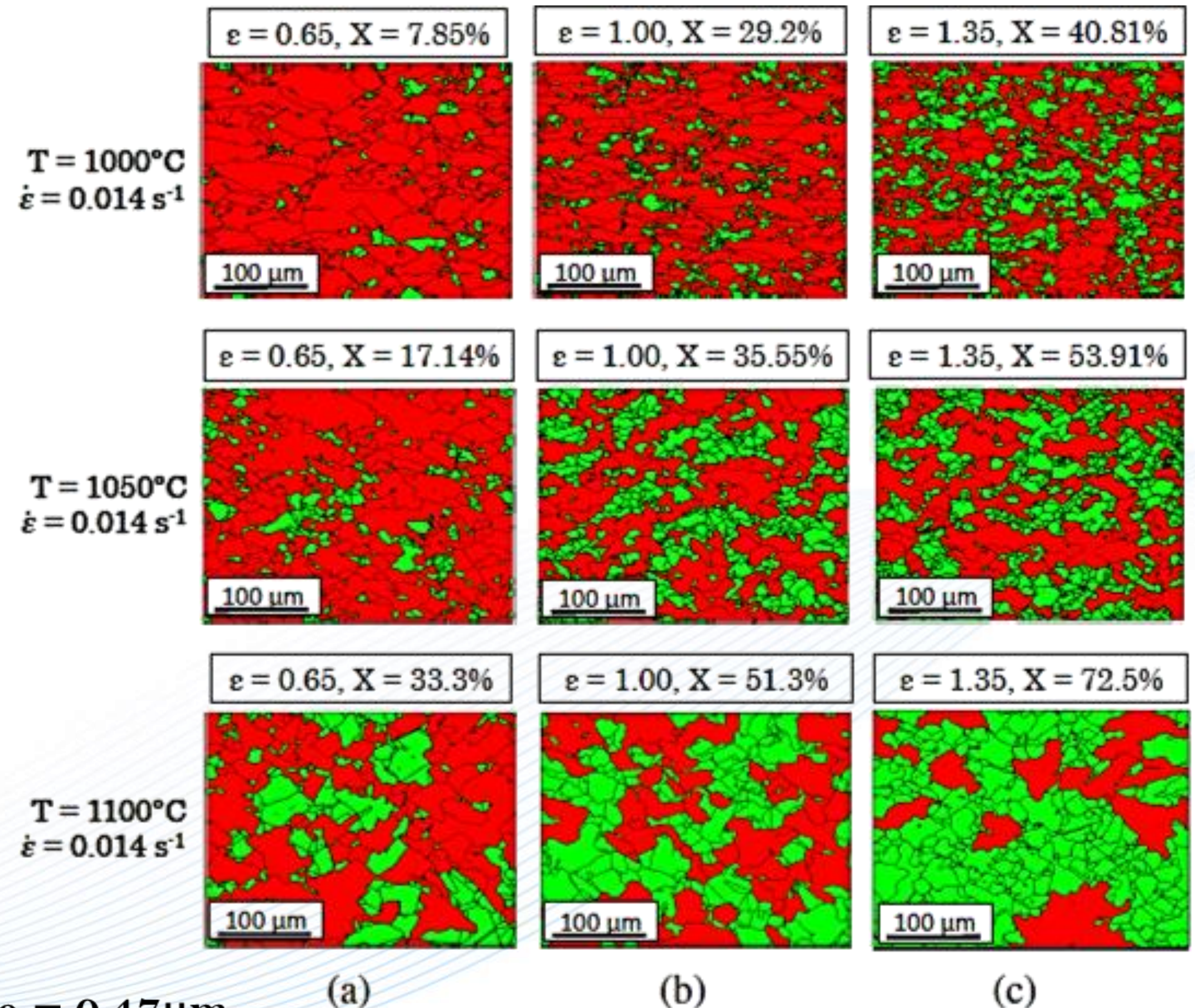

NR grains

RX grains

Acquisition step size = 0.47µm

The identification of δ and K_g is made in two steps :

1. Use of the Saltykov method to transform 2D distributions into 3D ones (Saltykov 1958)
2. Inverse analysis using BFGS inverse analysis algorithm from Python software

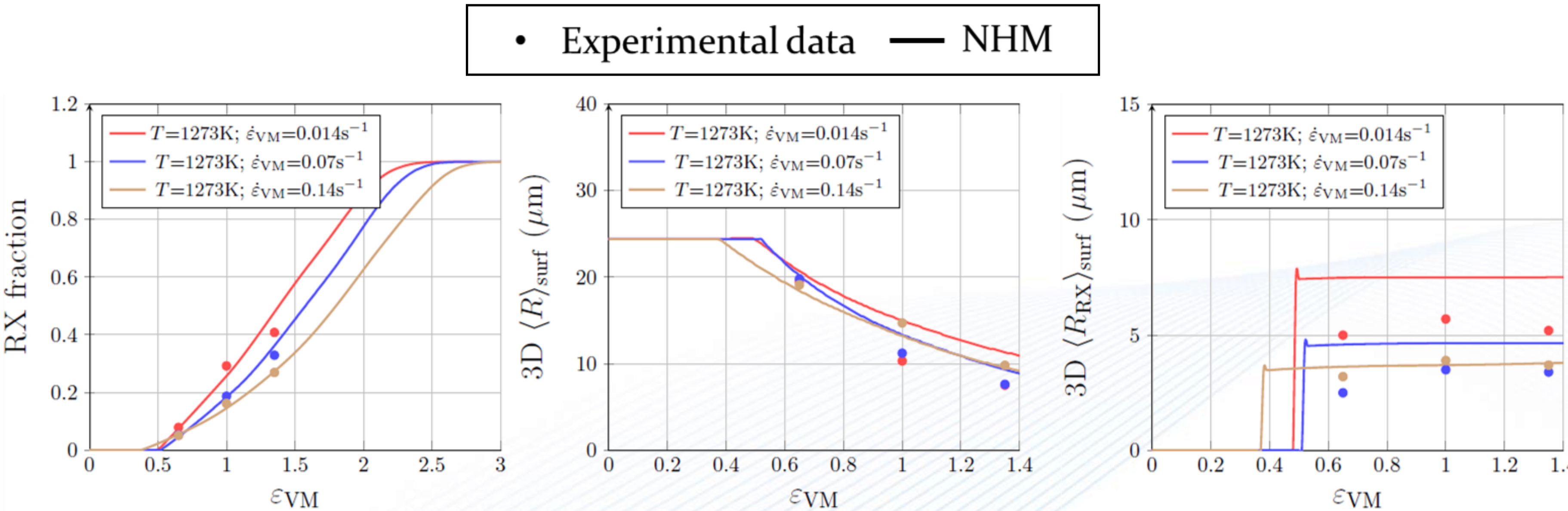

$$\dot{V} = K_g S_b \Delta t$$

$$v_{ij} = M * [\delta\tau(\rho_j - \rho_i) + \gamma(\frac{1}{R_j} - \frac{1}{R_i})]$$

Inverse analysis directly from mean field simulations to identify δ and Kg

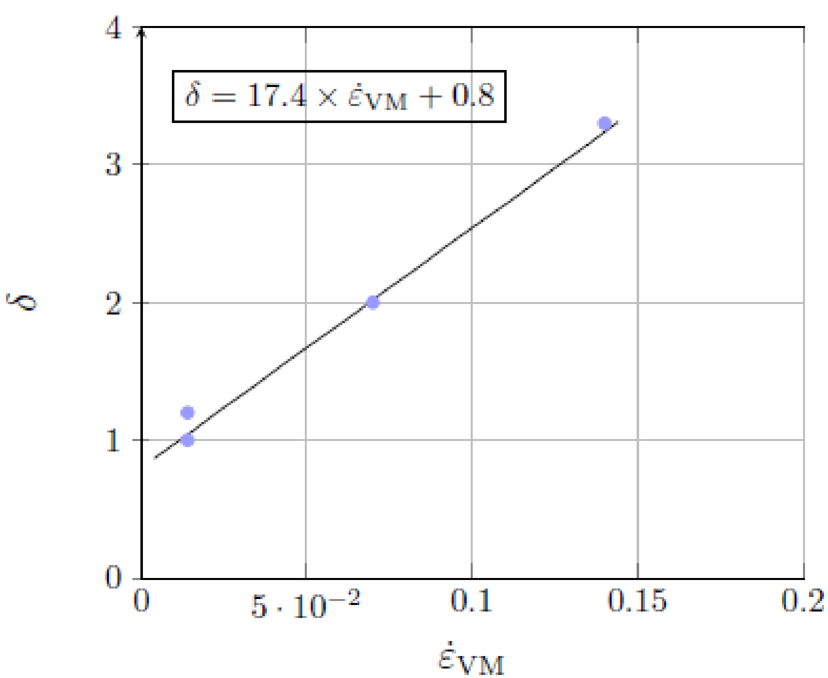

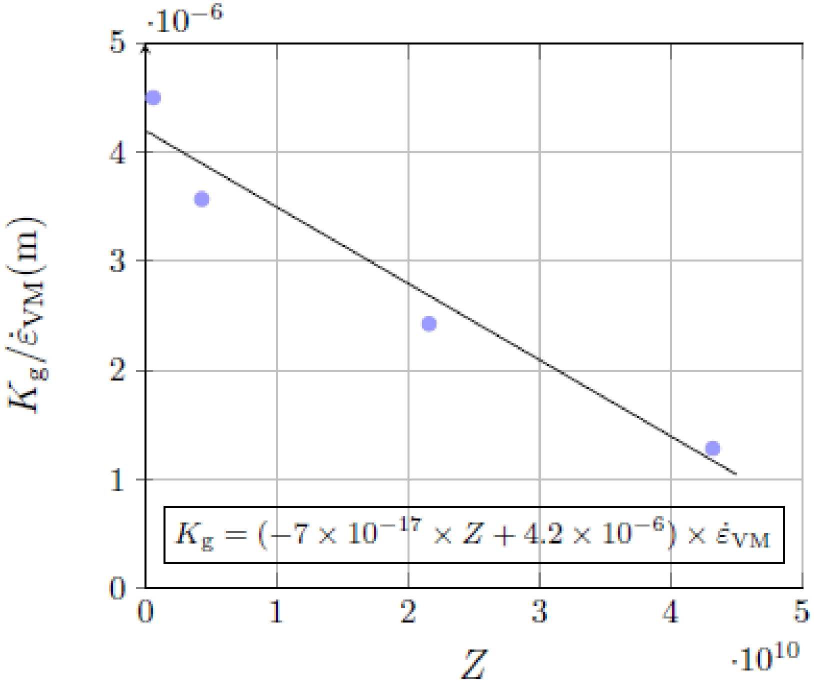

- The δ parameter (accounting for the dependence of mobility on strain rate) increases with strain rate
- The Kg parameter acounting for nucleation increases with temperature and strain rate
- Both dependence are in accordance with literature

Validation of the NHM :

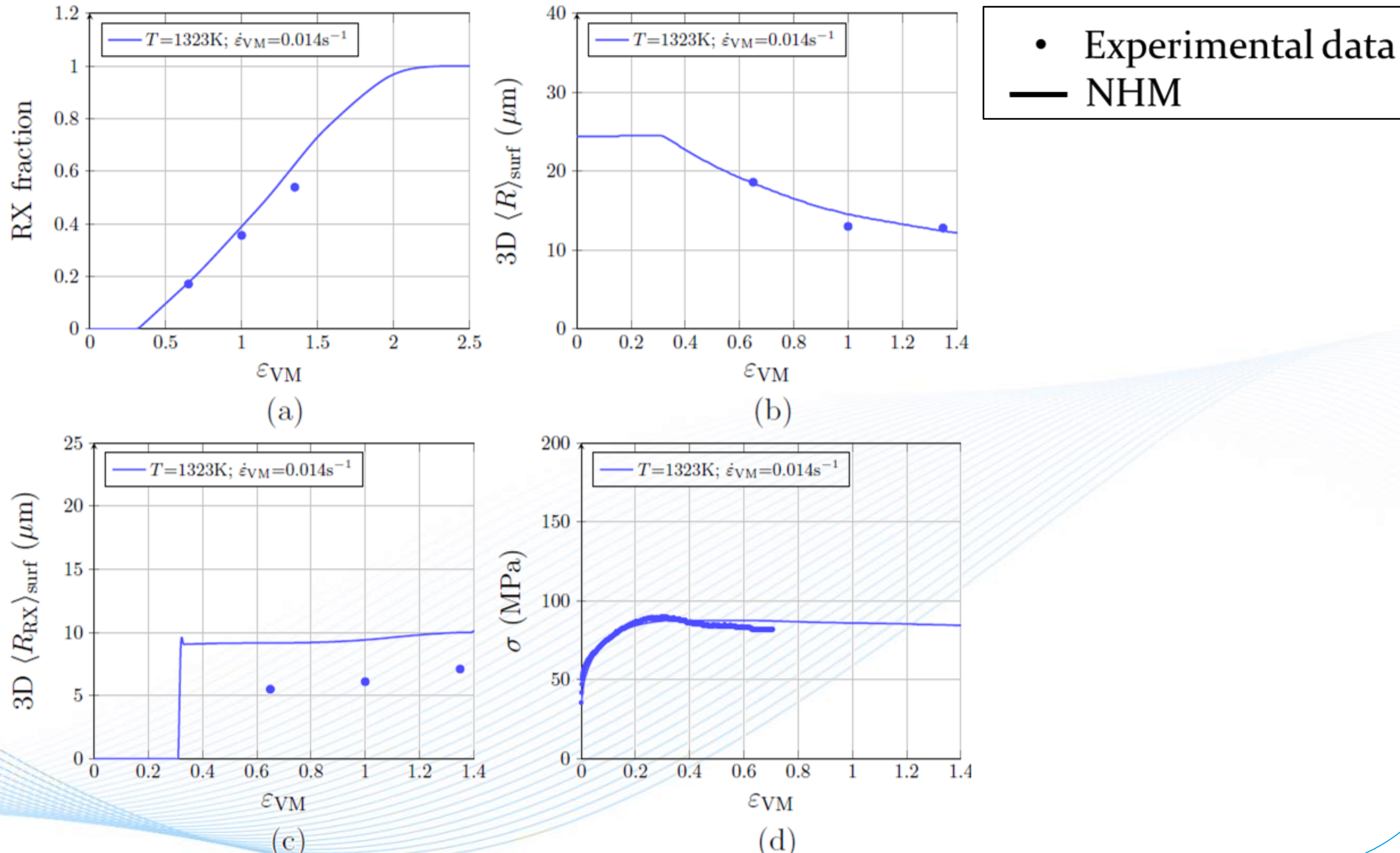

Comparisons of the three models :

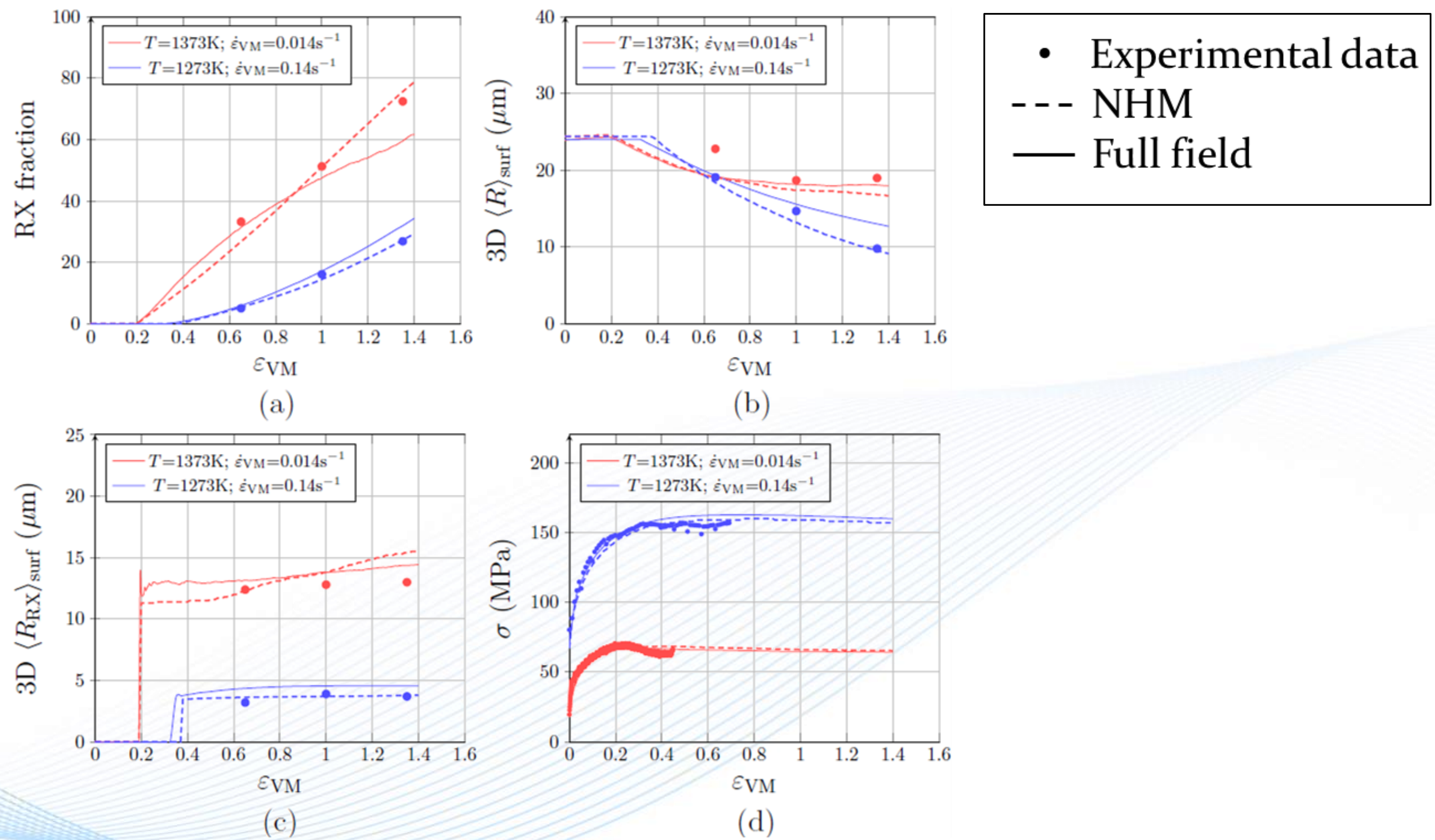

(a) (b) (c) (d)

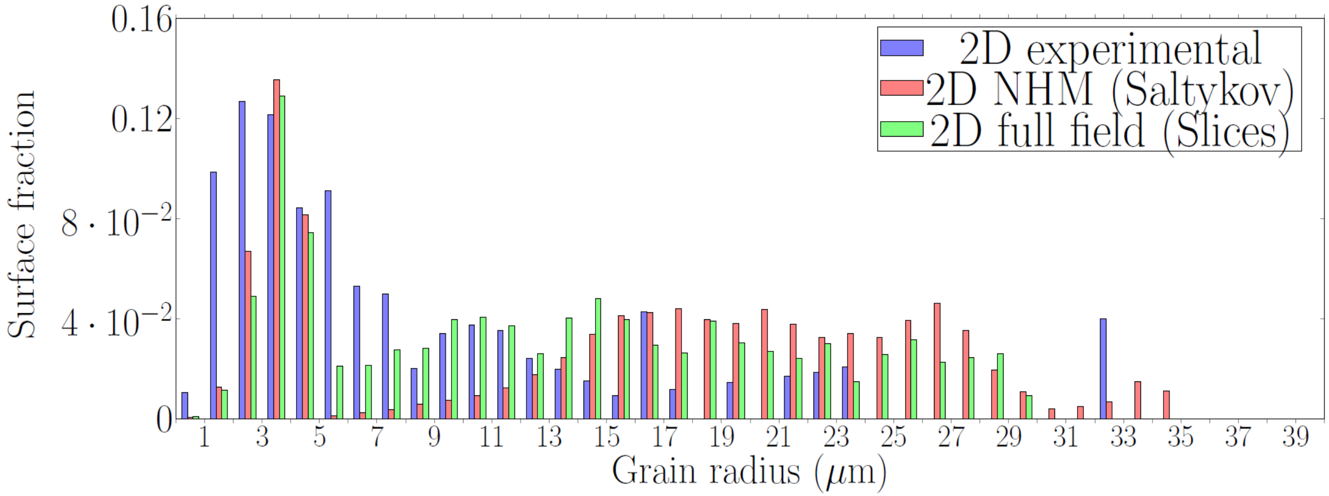

T=1273K, $\dot{\varepsilon}_{\mathrm{VM}}$=0.14s^{-1}, $\varepsilon_{\mathrm{VM}}$=1.35, X_{expe}=26.9%

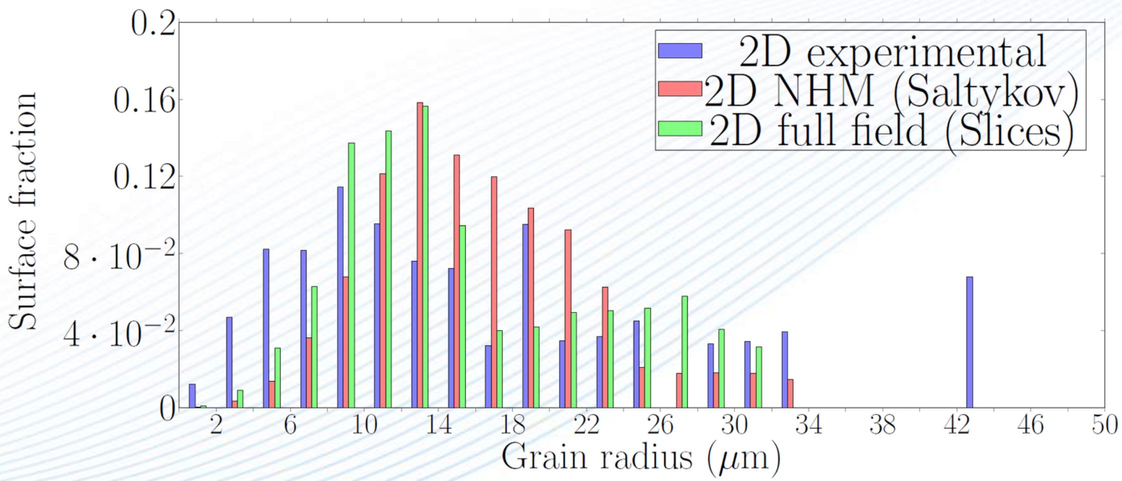

T=1373K, $\dot{\varepsilon}_{\mathrm{VM}}$=0.014s^{-1}, $\varepsilon_{\mathrm{VM}}$=1.35, X_{expe}=72.5%

Comparaisons of experimental EBSD maps and 2D slices from 3D full field simulations

$(T = 1273K, \dot{\varepsilon} = 0.014 s^{-1})$

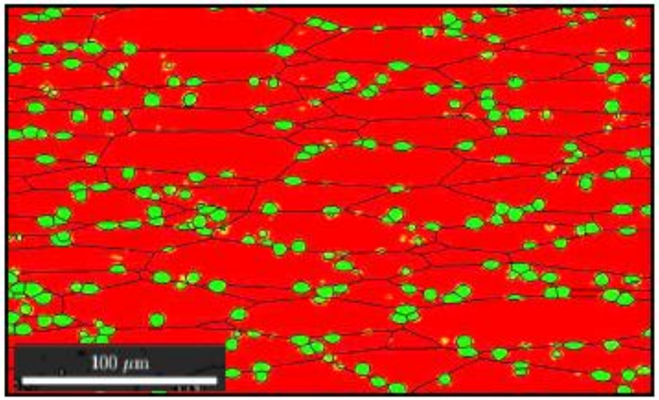

Full field, $\varepsilon_{VM} = 1$

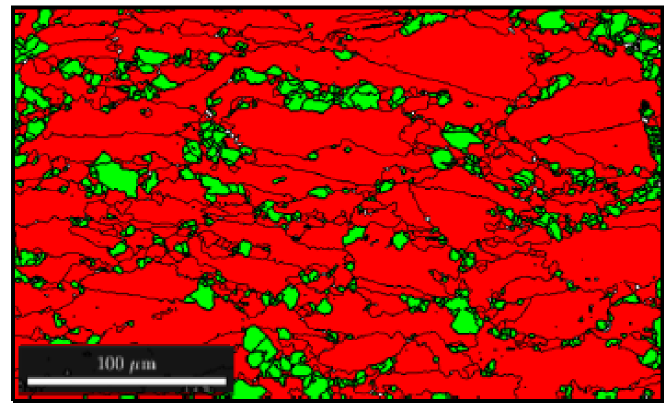

Experimental, $\varepsilon_{VM} = 1$

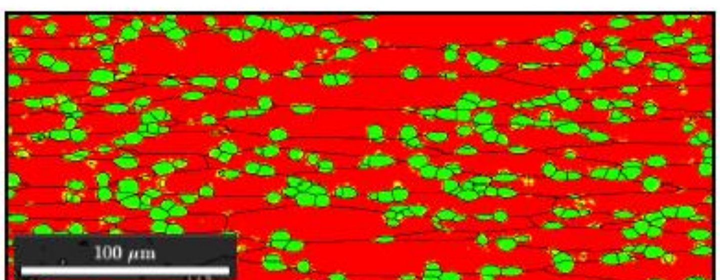

Full field, $\varepsilon_{VM} = 1.35$

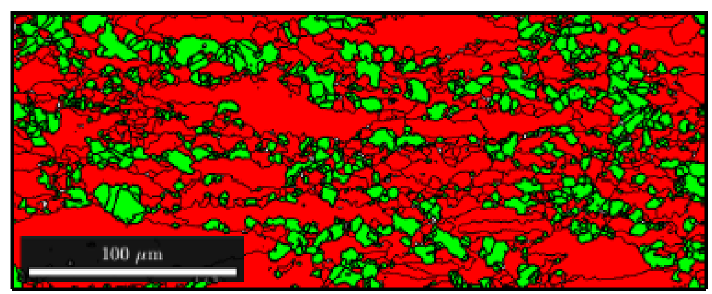

Experimental, $\varepsilon_{VM} = 1.35$

Final conclusions

- A new full field model aiming to model DRX and PDRX in 3D, for large deformation and with low computational cost was proposed. This model is already integrated into the DIGIMU® software package.
- With the help of full field simulations, a new mean field approach for modeling of DRX and PDRX was also proposed. This new approach tackles limitations of former mean field models, in particular concerning grain size distributions.
- An identification procedure applied on the 304L steel was proposed for these two models. This calibration method is based on stress-strain curves and microstructure quantities. After calibration, the predictions of these two models were validated for a new set of thermomechanical conditions.

Prospects related to this PhD work

- The full field model will be coupled with a crystal plasticity algorithm (PhD of David Ruiz) in order to tackle the assumptions made in analytical laws for strain hardening and recovery.
- Additional experimental investigations out of the considered range of thermomechanical conditions (1273-1373K and 0.01 and 0.1s^{-1}) need to be performed to check the consistency of the two models.
- An identification procedure must be proposed during the PDRX regime to identify the static recovery parameters K_s and check if static nucleation occurs.
- The identification procedure must be tested on other metals alloys (current works with partners of the DIGIMU consortium)

Prospects related to the DIGIMU software

- Consideration of anisotropic grain boundary energies.
[PhD, Julien Fausty (2016-2019)]

- Consideration of solid-solid phase transformations.
[PhD, Chau-Thuy Pham (2017-2020)]

- Improvement of the numerical framework.
[PhD, Sebastian Florez (2017-2020)]

- Modeling of second-phase particles and their growth/shrinkage.
[PhDs, Karen Alvarado and Romane Quere (2017-2021)]

- More explicit description of grain boundary mobility considered during simulations.
[PhD, Brayan Murgas (2018-2021)]

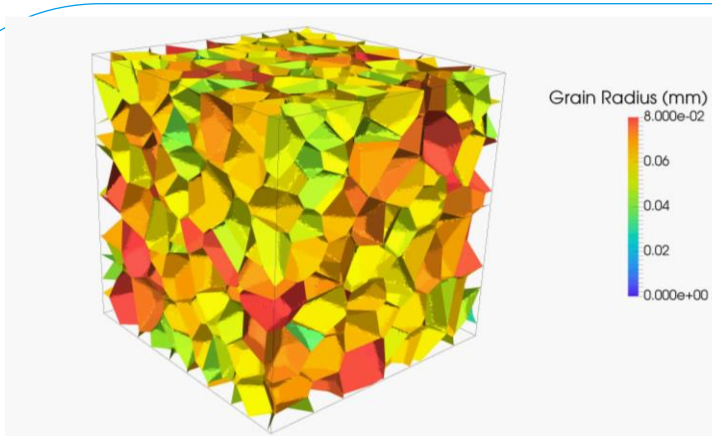

PhD Ludovic Maire

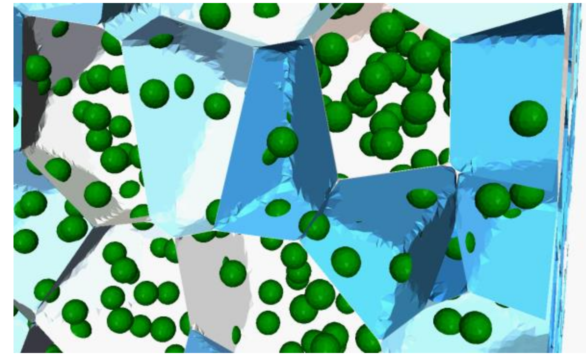

PhD Benjamin Scholtes

Many thanks for your attention

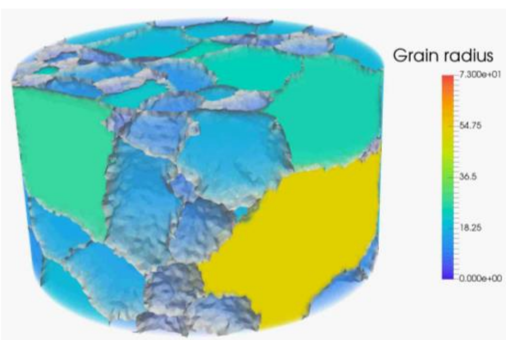

PhDs Benjamin Scholtes and Julien Fausty Collaboration with C. Krill and M. Wang

Marc Bernacki

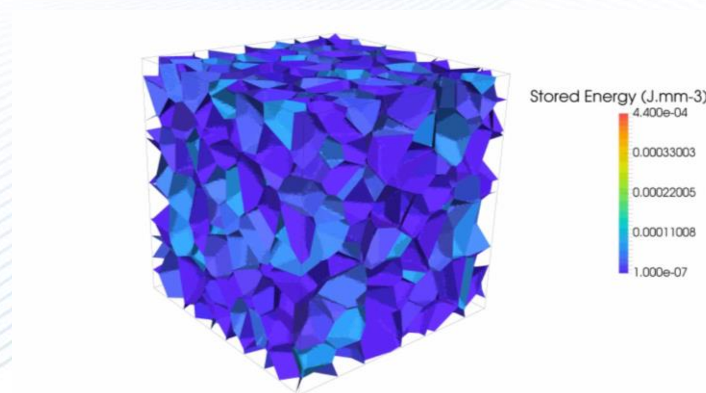

PhD Ludovic Maire

Two kinds of full field models

Stochastic approaches	Deterministic approaches
(e.g. Cellular Automata, Monte Carlo)	(e.g. Vertex, Phase-Field, Level-Set)

↗ Fast and well-suited with parallelization
→ Implementation
↘ polycrystal deformation
↘ Stochastic aspect

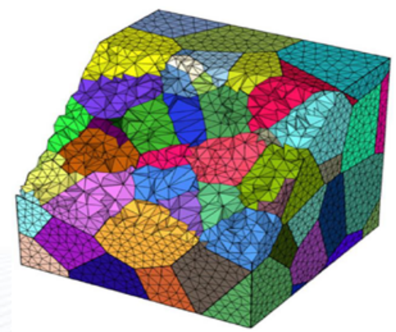

↗ Deterministic laws
→ polycrystal deformation
↘ Numerical cost

➢ A Level-Set method in a finite element framework is considered in this work

Ideal ratio between nucleus size and mesh size

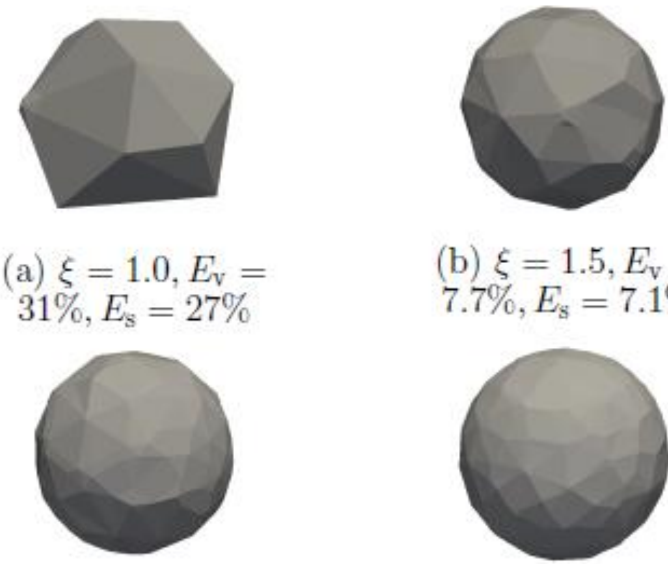

(a) $\xi = 1.0$, $E_v = 31\%$, $E_s = 27\%$

(b) $\xi = 1.5$, $E_v = 7.7\%$, $E_s = 7.1\%$

(c) $\xi = 2.1$, $E_v = 4.3\%$, $E_s = 4,3\%$

(d) $\xi = 2.6$, $E_v = 2.8\%$, $E_s = 2.5\%$

Fig. 3.5. *Four nuclei generated according to different mesh sizes. ξ corresponds to the ratio between the nucleus radius r_{cr} and the mesh size. E_v (resp. E_s) corresponds to the L^1 error between the volume (resp. surface) of the generated nucleus and the volume (resp. surface) of a sphere of same radius.*

Channel-Die compression test

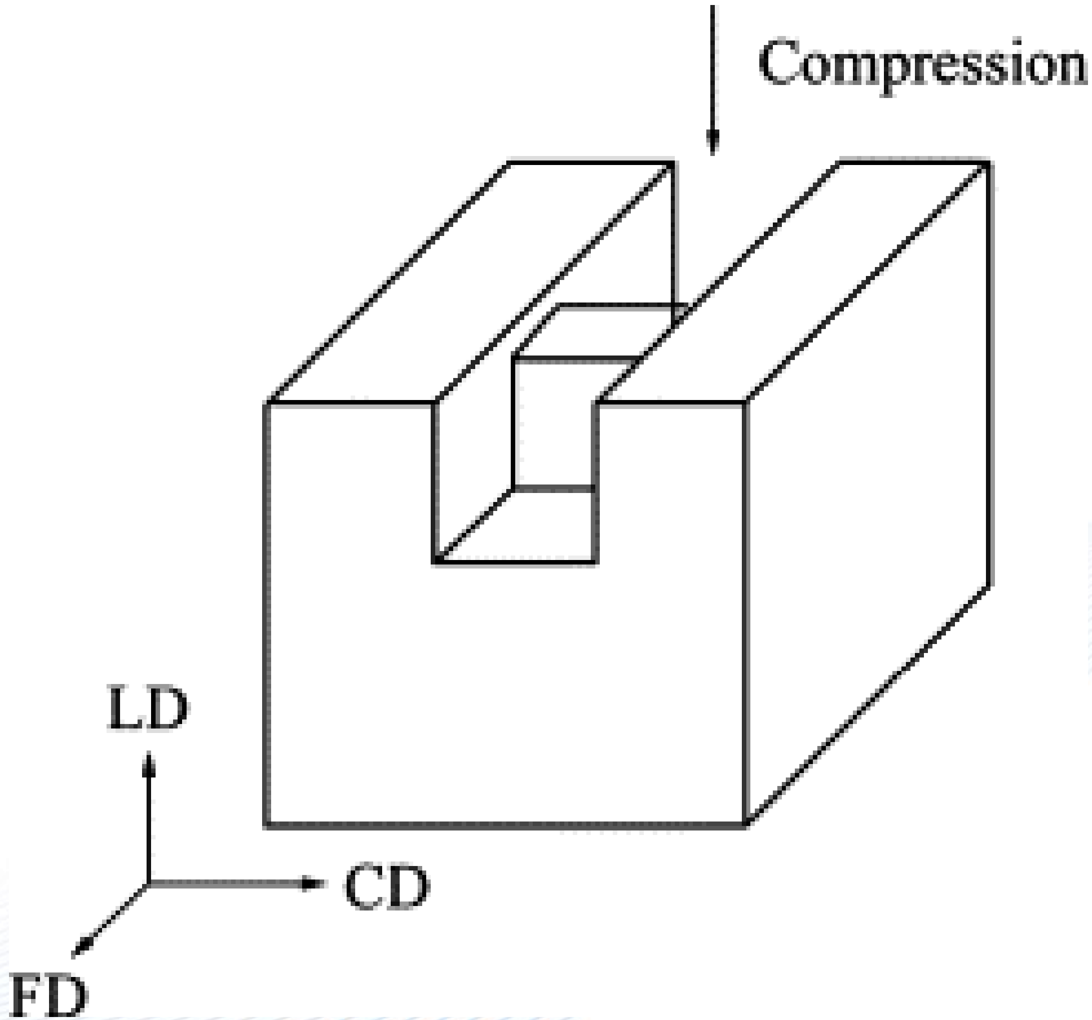

Futur extension of grain shape evolution

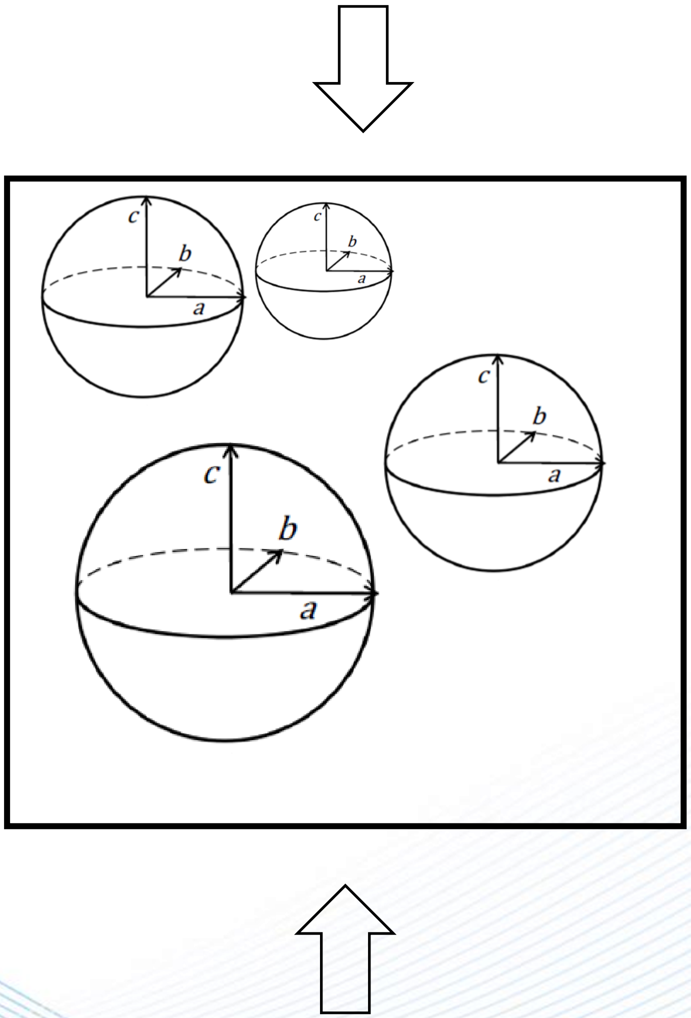

Futur extension of grain shape evolution

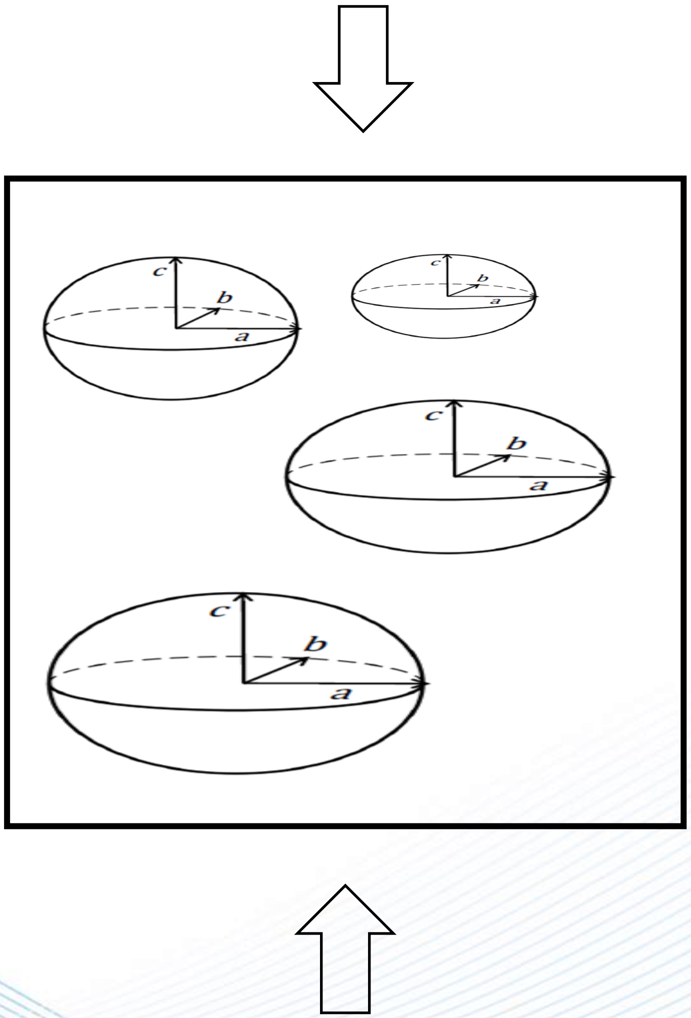

Futur extension of grain shape evolution

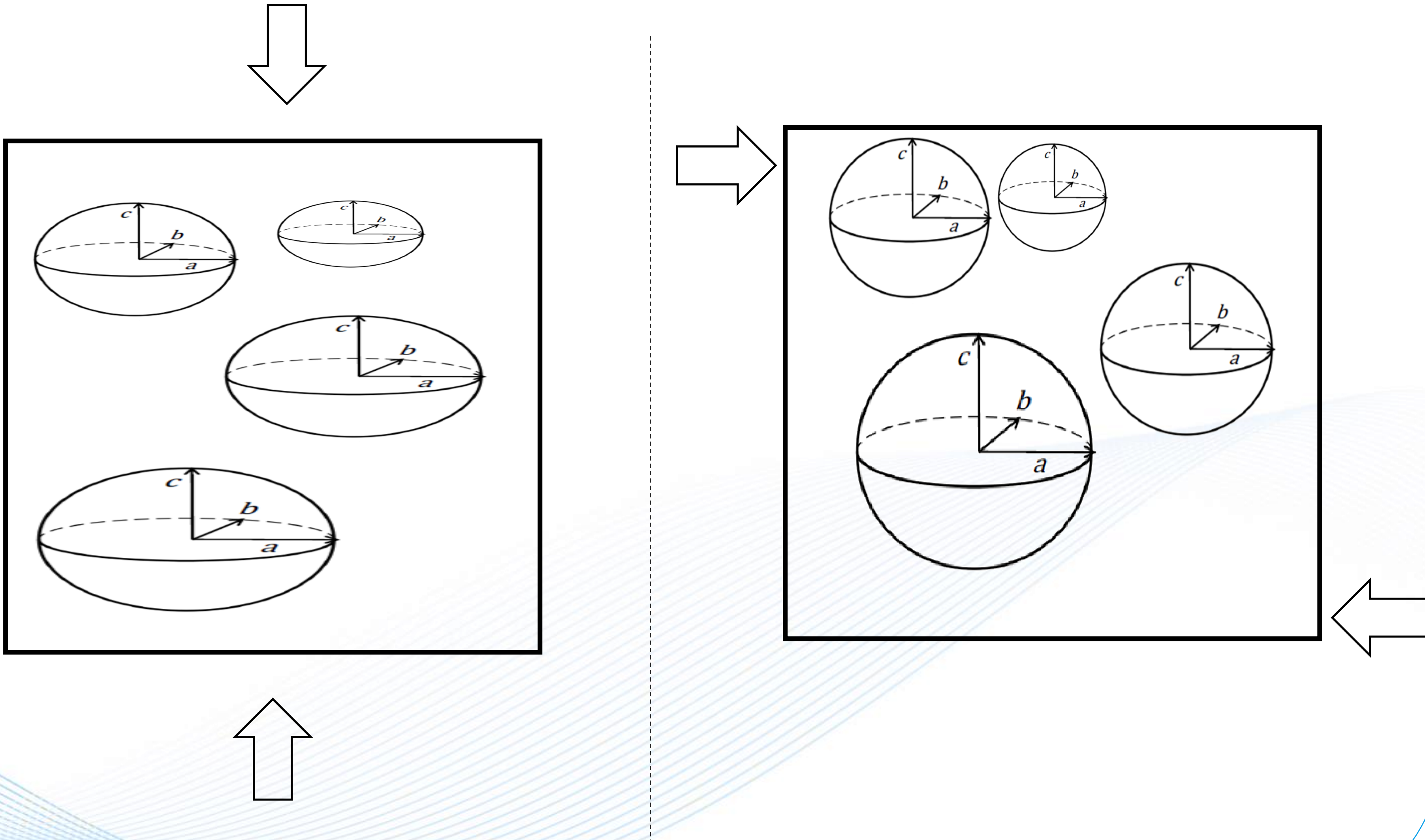

Futur extension of grain shape evolution

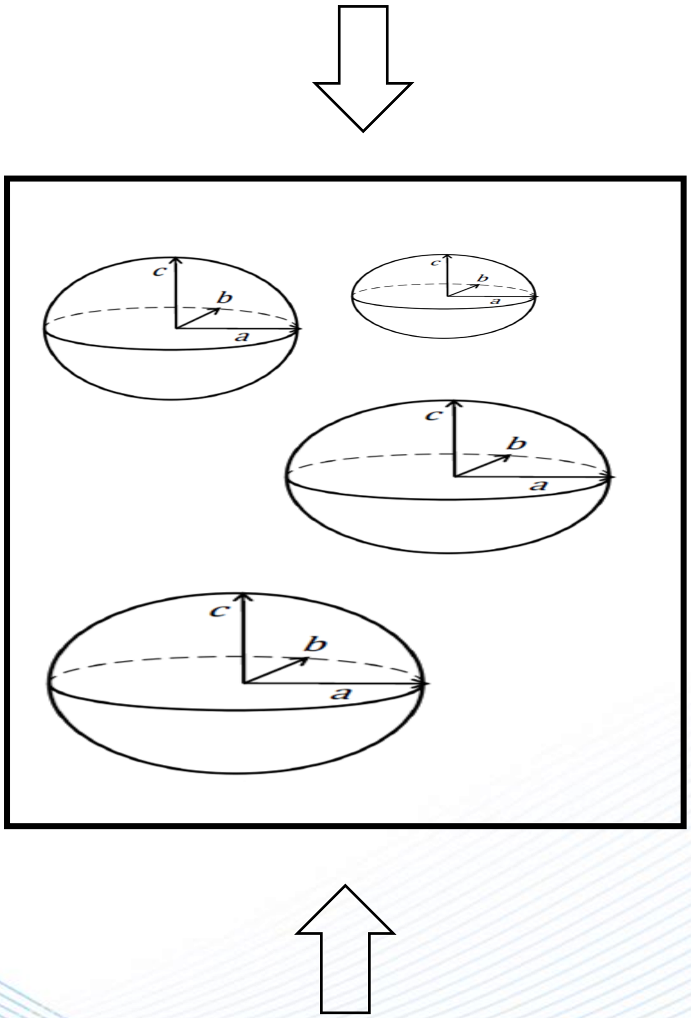

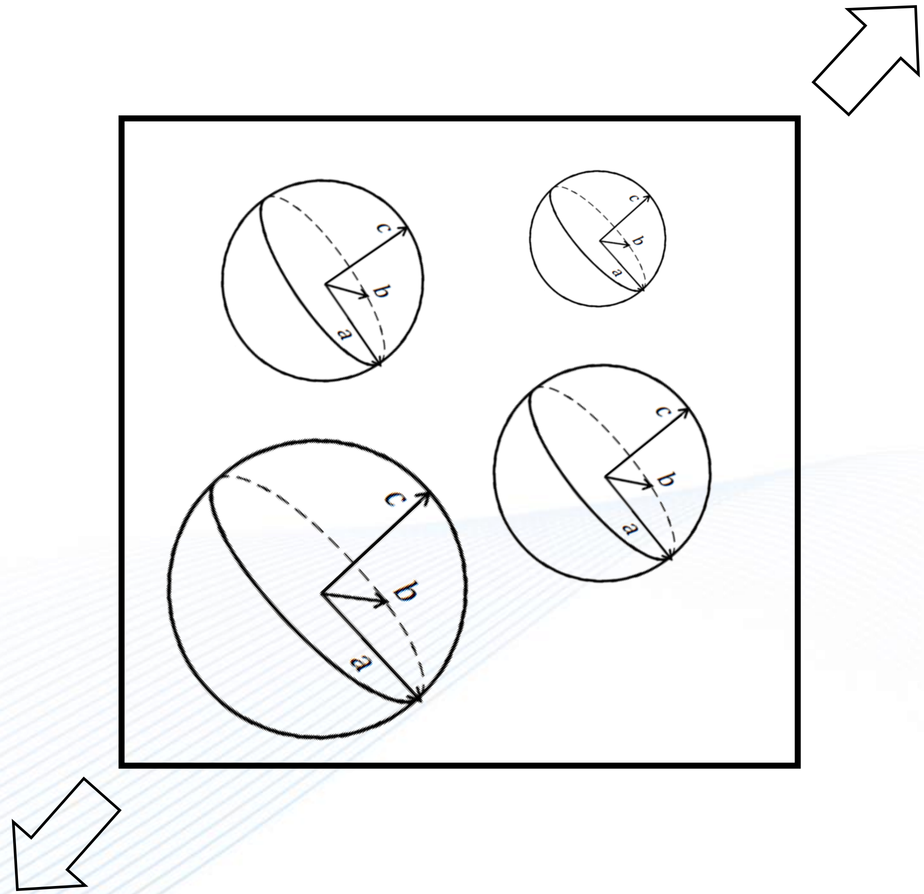

Futur extension of grain shape evolution

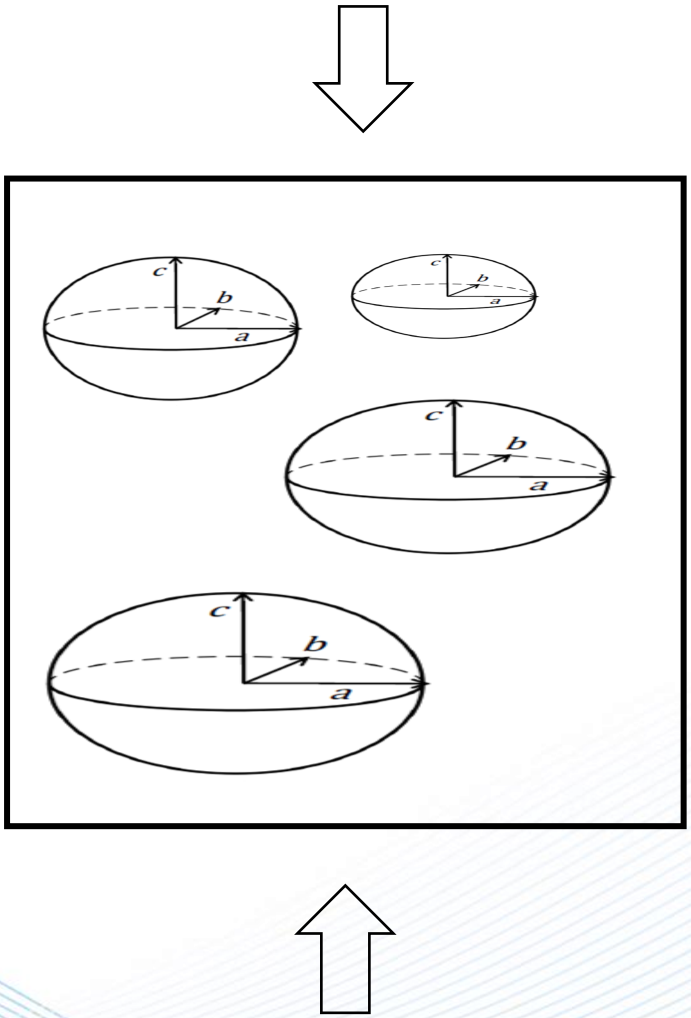

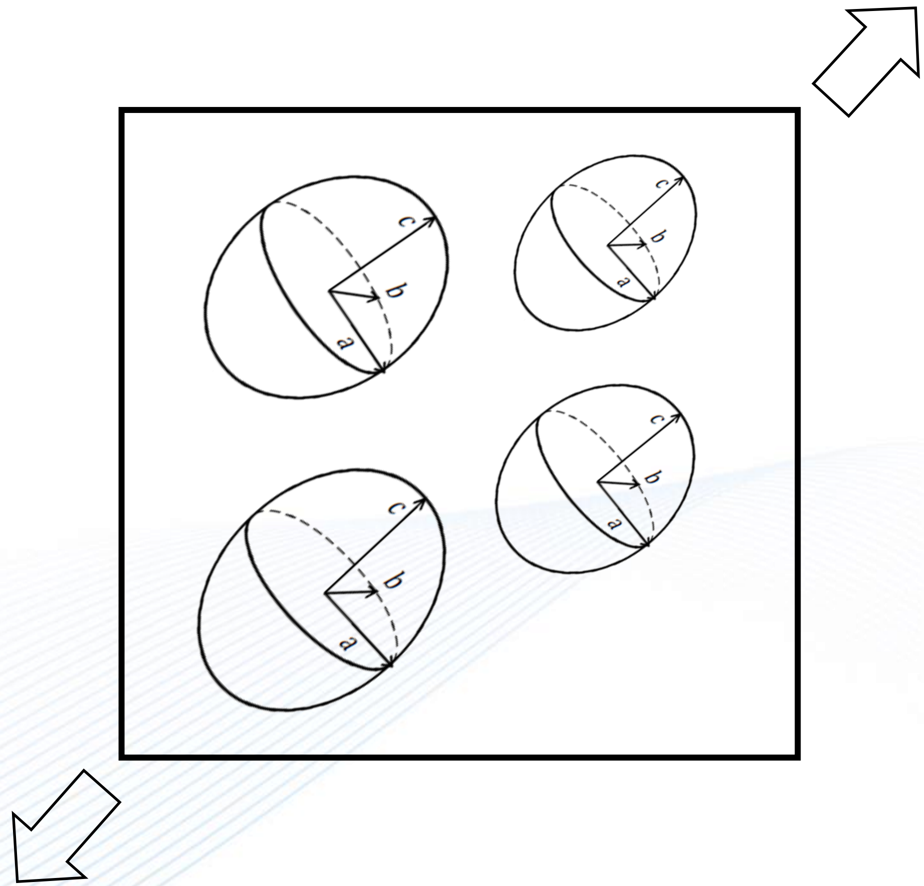

Futur extension of grain shape evolution

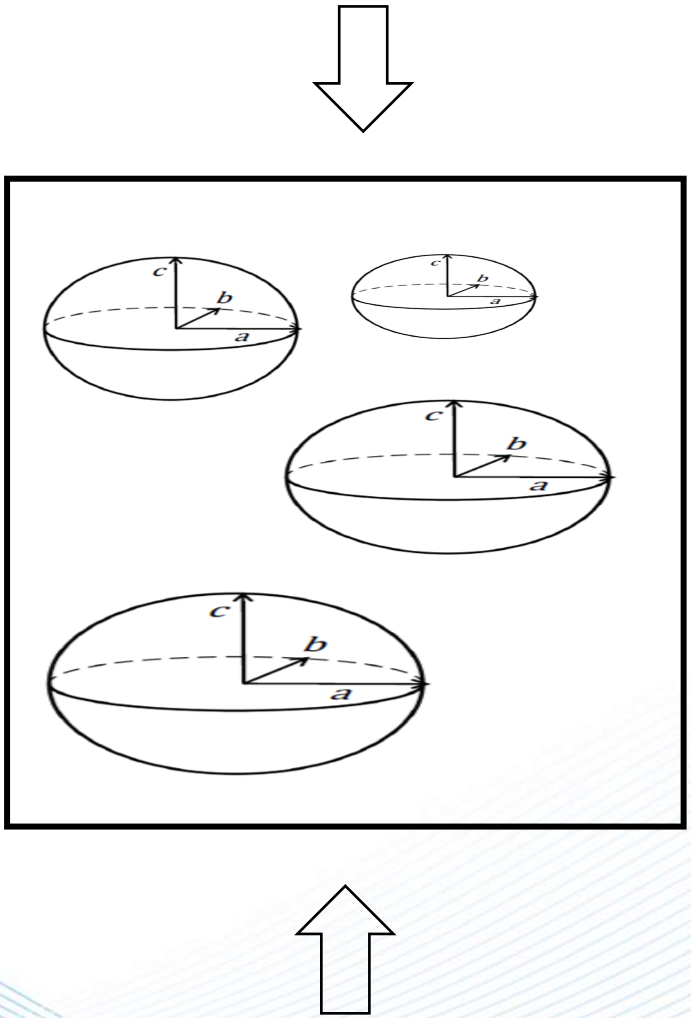

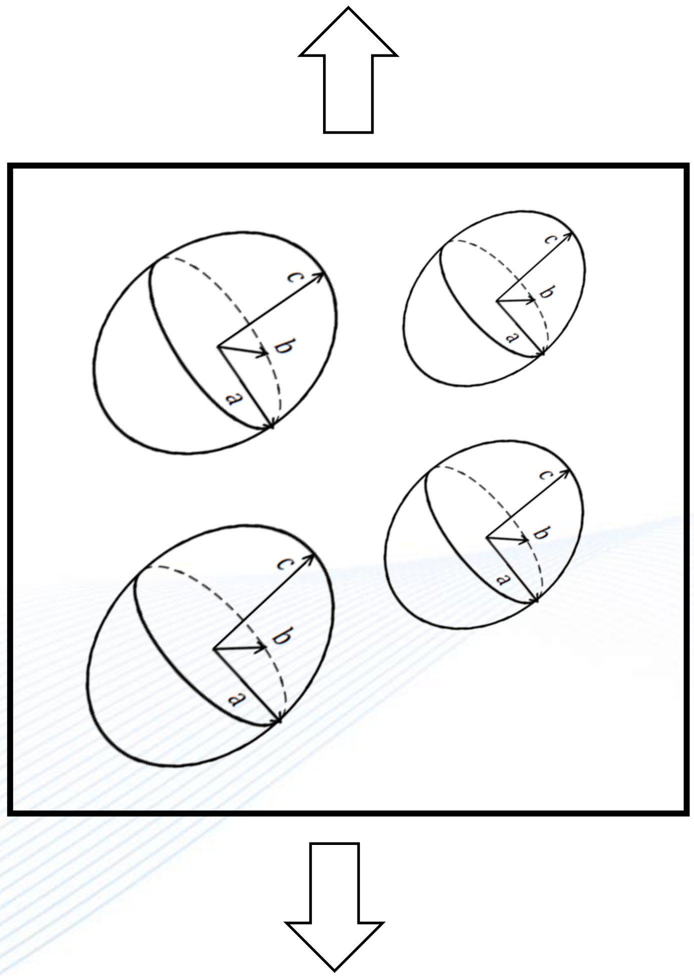

Futur extension of grain shape evolution

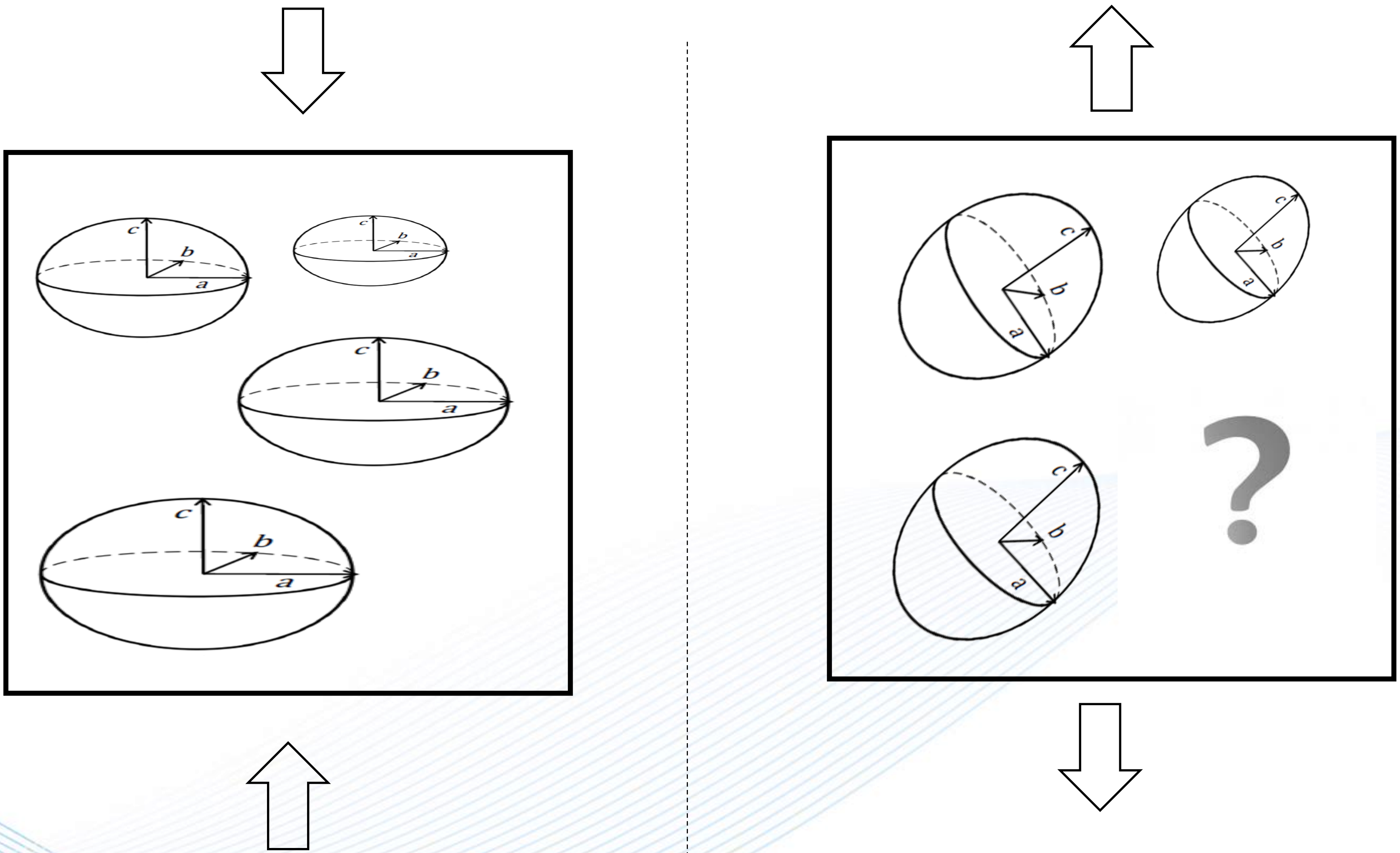

Idealized deformation step in the NHM

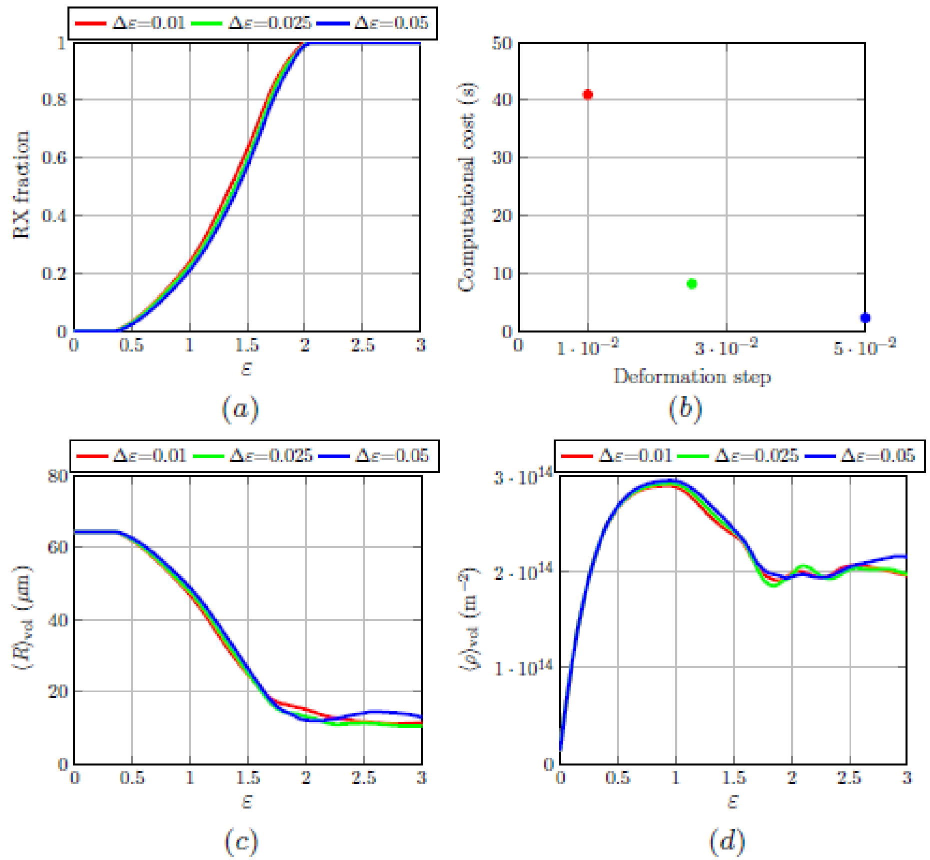

Fig. 4.12. *Sensitivity study of the deformation step on results obtained with the NHM: (a) recrystallized fraction (b) computational cost (c) mean grain radius (weighted by grain volume) (d) mean dislocation density (weighted by grain volume). Simulations were performed at a strain rate of* $0.01\,s^{-1}$ *and a temperature of 1273K.*

Considered in all NHM simulations

$\Delta\varepsilon = 0.025$

$\Delta t = \Delta\varepsilon / \dot{\varepsilon} = 0.025 / \dot{\varepsilon}$

To avoid prohibitive time steps due to low strain rates :

$\Delta t = \max(\Delta t\ ;\ 5s)$